energies

MDPI

Article

Towards Biochar and Hydrochar Engineering—Influence of Process Conditions on Surface Physical and Chemical Properties, Thermal Stability, Nutrient Availability, Toxicity and Wettability

Alba Dieguez-Alonso [1,*], Axel Funke [2], Andrés Anca-Couce [3], Alessandro Girolamo Rombolà [4], Gerardo Ojeda [5], Jörg Bachmann [6] and Frank Behrendt [1]

1 Institute of Energy Engineering, Technische Universität Berlin, Chair for Energy Process Engineering and Conversion Technologies for Renewable Energies, Fasanenstr. 89, 10623 Berlin, Germany; frank.behrendt@tu-berlin.de

2 Institute of Catalysis Research and Technology (IKFT), Karlsruhe Institute of Technology, Hermann-von-Helmholtz-Platz 1, 76344 Eggenstein-Leopoldshafen, Germany; axel.funke@kit.edu

3 Institute of Thermal Engineering, Graz University of Technology, Inffeldgasse 25b, 8010 Graz, Austria; anca-couce@tugraz.at

4 Department of Chemistry "Giacomo Ciamician", C.I.R.I. Energia Ambiente and C.I.R.S.A., Università di Bologna, Ravenna Campus, Via S. Alberto 163, 48123 Ravenna, Italy; alessandro.rombola@unibo.it

5 Ecological and Forestry Applications Research Centre (CREAF), 08193 Cendanyola del Vallès, Spain; g.ojeda@creaf.uab.cat

6 Institute of Soil Science, Leibniz University of Hannover, Herrenhaeuser Str. 2, 30419 Hannover, Germany; bachmann@ifbk.uni-hannover.de

* Correspondence: alba.dieguezalonso@tu-berlin.de; Tel.: +49-(30)-314-24381

Received: 31 December 2017; Accepted: 11 February 2018; Published: 27 February 2018

Abstract: The impact of conversion process parameters in pyrolysis (maximum temperature, inert gas flow rate) and hydrothermal carbonization (maximum temperature, residence time and post-washing) on biochar and hydrochar properties is investigated. Pine wood (PW) and corn digestate (CD), with low and high inorganic species content respectively, are used as feedstock. CD biochars show lower H/C ratios, thermal recalcitrance and total specific surface area than PW biochars, but higher mesoporosity. CD and PW biochars present higher naphthalene and phenanthrene contents, respectively, which may indicate different reaction pathways. High temperatures (>500 °C) lead to lower PAH (polycyclic aromatic hydrocarbons) content (<12 mg/kg) and higher specific surface area. With increasing process severity the biochars carbon content is also enhanced, as well as the thermal stability. High inert gas flow rates increase the microporosity and wettability of biochars. In hydrochars the high inorganic content favor decarboxylation over dehydration reactions. Hydrochars show mainly mesoporosity, with a higher pore volume but generally lower specific surface area than biochars. Biochars present negligible availability of NO_3^- and NH_4^+, irrespective of the nitrogen content of the feedstock. For hydrochars, a potential increase in availability of NO_3^-, NH_4^+, PO_4^{3-}, and K^+ with respect to the feedstock is possible. The results from this work can be applied to "engineer" appropriate biochars with respect to soil demands and certification requirements.

Keywords: pyrolysis; hydrothermal carbonization; biochar engineering; porosity; nutrients; polycyclic aromatic hydrocarbon (PAH)

1. Introduction

The definitions of biochar provided by the European Biochar Certificate (EBC) [1] and the IBI (International Biochar Initiative) Biochar Standards [2] address biochar properties requirements for its application, as well as methodological standards to assess them, but they do not describe in detail the production process and its influence on biochar properties. As an example, the EBC considers mainly pyrolysis as the process to produce biochar, including gasification as part of the pyrolysis technology spectrum. However, the IBI Biochar Standards consider all forms of thermochemical conversion with limited presence of oxygen as appropriate technologies to produce biochar. Therefore, hydrothermal carbonization (HTC) could be included as well. In recent years, a lot of research has been done in the field of biochar to understand the impact of process conditions on biochar properties, as well as biochar dynamics once applied to soil and, consequently, its potential positive and/or negative impacts on crops, environment and soil. However, as Abiven et al. [3] pointed out, it is necessary to develop tailor-made biochar systems according to individual applications, taking into account soil type, climate and social environments, instead of considering biochar as an universal soil enhancer. Besides, biochar can have other applications, such as its use for soil and water remediation through the adsorption and immobilization of organic and inorganic contaminants [4–7]. Within its agronomic use, and according to a review by Mohan et al. [8], biochar can potentially increase nutrient availability (direct and indirect pathways), water retention, soil organic matter, microbial activity and crop yields. This may contribute to a reduction in nutrient leaching, fertilizer demand or emissions [9–11].

- Direct biochar contribution to nutrient availability relies on the macro- and/or micronutrients that biochar contains and their availability [5,9,10]. This is strongly dependent on the composition of the initial feedstock [10] and on the pyrolysis conditions. High retention of alkali species and P is reported for pyrolysis temperatures below 600–700 °C and low heating rates [12–15], with increase in total, soluble and exchangeable base cations with increasing process severity [13]. However, Uchimiya et al. [16] showed that NaOH-EDTA extractable P increased at 300–350 °C pyrolysis temperature and decreased at higher temperatures for plant and manure biochars. Hossain et al. [17] showed that total N content and N availability decreased with increasing pyrolysis temperature in wastewater sludge biochars.
- Indirect contribution to nutrient availability relies on the capacity of biochars to retain applied nutrients, potentially reducing leaching and increasing fertilizer-use efficiency, on their liming effect or on their impact on other soil properties, such as the potential increase in water-holding capacity, among others, as reviewed by Chan and Xu in [10]. Biochars nutrient retention capacity is associated to their surface charge and surface physical properties as stated by Chan and Xu in [10].
- Biochar surface charge will impact the biochar capacity to adsorb positively or negatively charged nutrients. The cation exchange capacity (CEC) is a measure of the biochar capacity to retain positively charged species, mainly through electrostatic interactions [7,18]. Budai et al. [19] reported that CEC is influenced by different factors, with no clear dominance. These may include: the presence of negatively charged oxygen-containing functional groups on the biochar surface, such as carboxylate (from carboxylic acid) and hydroxyl functional groups [13,18–20], which are reported to decrease with increasing conversion temperature [13,18,19,21,22]; the pH of the solution [18]; the content and composition of the inorganic fraction [23,24]. Values for biochars CEC and its dependence on process conditions and feedstock vary significantly in literature [18,19,24]. Biochars anion exchange capacity (AEC) is scarcely reported in literature [20], with studies even showing negligible AEC [18]. Little is known about the origin of AEC on the surface of biochar [20]. However, due to the relevance of this topic, especially towards the reduction in negatively charged nutrients leaching, such as phosphates and nitrates, plenty of recent research activity focuses on the modification of biochar surfaces to enhance their capacity or adsorb such species.

- Biochar specific surface area and pore volume increase with pyrolysis temperature [19,21,25] up to approximately 600–700 °C, when further ordering of the biochar structure may lead to a decrease in surface area [19,25]. Mainly micropores contribute to the specific surface area in biochars [21]. Other process parameters, such as biomass composition, specially inorganic species content, heating rate and pressure can have also a significant impact on porosity development [26,27]. Surface area and pore network may impact biochar adsorption capacity due to the influence on accessibility [18] and availability of adsorption sites.
- With respect to water retention, this depends on both the physical and chemical surface properties of biochar. The nature of surface functional groups impacts the hydrophobic/hydrophilic behavior or biochars [20]. As reported by Schimmelpfenning et al. [21], polar functional groups on the biochar surface may increase the uptake of water due to electrostatic interactions and hydrogen bonds. Their reduction can lead to higher hydrophobic caracter [28]. Hagemann et al. [29] reported that biochar-water interactions enhancement, leading to higher nutrient retention, can be achieved with higher mesoporosity, redox-active sites and hydrophilicity on the surface of biochars.
- Biochars pH is of high relevance for its application in soil, since it determines not only its potential liming effect, but it also has an influence on other properties, such as CEC, water holding capacity or adsorption capacity for different nutrients or heavy metals [18,30].

Consequently, in order to achieve the capacity of "engineering biochar", not only further knowledge of the mechanisms behind biochar interactions in soil (including quantification and durability of the impact and variability in response) [9,31] is required, but also a deeper mechanistic understanding of the influence of conversion process and feedstock on biochar properties and its function in soil. This is a complex issue due to the highly relevant influence of (1) feedstock, (2) type of process, and (3) process parameters on biochar characteristics, as briefly introduced.

For pyrolysis, temperature and feedstock properties are the main process parameters under consideration when investigating the influence of conversion process on biochar properties. However, other process variables such as inert gas flow rate, heating rate, particle size, atmosphere and pressure can dramatically change biochar properties as well [26,32,33]. Furthermore, with HTC the chemical pathways involved differ significantly from those of pyrolysis. The different nature of these chemical reactions open up the potential to design carbon materials with a variety of interesting functionalities [34].

Comparison of chars produced from pyrolysis (termed biochars in the following) and chars produced from HTC (termed hydrochars in the following) has been previously done in literature, as summarized in Table 1. Huff et al. [35] reported higher O/C ratios for hydrochars than for biochars, as well as a significantly higher CEC, which, however, did not correlate well with the capacity of these chars to adsorb organic compounds (methylene blue). Budai et al. [19] showed that volatile matter and H/C and O/C ratios can be good parameters to determine the carbonization degree, irrespective of conversion process and feedstock, but poor predictors for agronomic properties (SSA and CEC). Liu et al. [28] reported that HTC creates oxygen-containing functional groups on the hydrochar surface with respect to the feedstock, while pyrolysis reduces their presence. Both biochar and hydrochar develop a rough surface and pore structure and are able to remove metal species from wastewater, such as copper, although different adsorption mechanisms can be responsible [28]. Based on a wide comparison of biochars, produced through different methods, and hydrochars, quality indicators for biochar production were suggested, such as H/C ratios below 0.6, O/C ratios below 0.4 and black carbon content higher than 15% (based on C), to ensure stability in soil [21]. Moreover, BET SSA higher than 100 $m^2\ g^{-1}$ and PAHs content according to the precautionary values defined by the German federal soil protection ordinance ("Bundesbodenschutzverordnung") should be achieved [21]. Regarding chemical structure, it was shown that while biochar is mostly aromatic, with small traces of alkyl carbons, hydrochars contain mostly alkyl moieties [36]. This was further confirmed in [37], where it was also reported that hydrochars have higher nutrient retention capacity than biochars. At the same time, both were within the EBC [1] recommended limits for PAHs content [37]. It was concluded

that conversion conditions strongly affect the char properties and that, while biochar standards are described in the EBC [1], hydrochars need their own directive [37]. In [36], it was also shown that the aromatic cluster size of biochar is larger than the one of hydrochar. Furthermore, acid prewashing and water and acetone washing can change the chemical structure of hydrochars [36]. Genotoxic and phytotoxic risk assessment showed hydrochars to be phytotoxic, inhibiting germination, although this effect could be eliminated with biological post-treatment [38]. Moreover, hydrochar is less suitable for long-term C sequestration in comparison to biochar, due to a lower stability, but it can deliver essential nutrients, having therefore potential for soil amelioration [39].

The objective of the present work is to contribute to the comparison between biochars and hydrochars by investigating the influence of conversion process conditions and feedstock on relevant properties. For this purpose, biochars and hydrochars were produced from two biomass feedstocks with varying mineral content (pine wood and corn digestate). Biochar was produced by pyrolysis in a fixed bed reactor at two maximum conversion temperatures (400 and 600 °C) and two inert gas flow rates (20 and 40 NL min^{-1} of N_2). Hydrochars were produced by HTC in a batch autoclave at two conversion temperatures (200 and 240 °C), two residence times (10 and 360 min) and with and without water washing after production (3 and 6 times). Together with primary characterization properties, such as proximate and elemental analyses, other characteristics, which can contribute to the understanding of biochar and hydrochar behavior once applied to soil, are analyzed: pH, acidic surface functional groups, pore size distribution with N_2 and CO_2 adsorption, nutrient availability, thermal stability, PAHs content and wettability.

Comparing the objectives of the present work and the previously reviewed literature, this study introduces a more detailed analysis on (1) the influence of conversion process parameters and (2) the characterization of products properties. With respect to process conditions, temperature, time and water washing have been chosen for HTC because very little data is available in the above mentioned publications regarding their combined influence on hydrochars. Moreover, the influence of inert gas flow rate in pyrolysis, and therefore the retention time of volatiles in the bed, is a novelty in this comparative study. This work represents a fundamental characterization of char produced under different and relevant process conditions and, therefore, issues regarding the energetic costs associated with inert gas flow rates, process temperatures or residence times cannot be evaluated based on these laboratory scale results. Furthermore, beyond the investigated product properties in the reviewed literature, a deep analysis is performed for the first time on the porous structure of both biochars and hydrochars combining N_2 and CO_2 adsorption, as well as research and comparison on nutrient availability and wettability. Finally, the results are analyzed from a conversion process perspective, in order to achieve an advance in the state-of-the-art of the "engineering biochar" concept.

Table 1. Summary of literature studies comparing biochars and hydrochars. CEC: cation exchange capacity, FTIR: Fourier-transform infrared spectroscopy, SSA: specific surface area, SEM: scanning electron microscopy, EDS: energy-dispersive X-ray spectroscopy, CT: CarbonTerra (Augsburg, Germany), BC: Black-Carbon (Barrit, Denmark), AGT: Advanced Gasification Technology (Arosio, Italy).

Authors	Process Conditions	Feedstock	Methods
Budai et al. [19]	Biochars from slow pyrolysis (235–800 °C), flash carbonization char (600 °C) and hydrochars (230 °C for 6 h)	Corncob and miscanthus	Proximate and elemental (CHNO) analyses, pH, CEC, SSA with N_2 adsorption
Schimmelpfennig and Glaser [21]	Biochars from slow pyrolysis (Pyreg unit) (550 °C), hydrochars (200 °C), rotary kiln biochars (350–550, 750 °C), gasification biochars (800 °C), traditional kiln biochars (350 °C), other biochars (350, 500, 650, 800 °C)	Wood, animal meal, sugar cane/beet, wheat, bamboo, maize, rice hulls, peanut shells, sewage sludge, walnut shells, girasol, coconut shells, lop, bark/needles	Elemental (CHNO) analysis, black carbon content, SSA with N_2 adsorption, PAHs content
Liu et al. [28]	Biochars from slow pyrolysis (700 °C), hydrochars (300 °C for 20 min)	Pine wood	Proximate and elemental (CHNO) analyses, Boehm titration, pH, FTIR spectroscopy, surface morphology with SEM, SSA and micro-, meso- and macropores volume with N_2 adsorption, copper removal capacity (adsorption) from wastewater
Huff et al. [35]	Biochars from slow pyrolysis (300, 400 and 500 °C) and hydrochars (300 °C for 30 min)	Pine wood, peanut shell and bamboo	Proximate and elemental (CHN) analyses, methylene blue adsorption, CEC, FTIR spectroscopy
Cao et al. [36]	Biochars from slow pyrolysis (620 °C) and hydrochars (with acid prewashing and water and acetone washing) (250 °C for 20 h)	Swine-manure	Major chemical structural components with Quantitative ^{13}C Direct Polarization/Magic-Angle Spinning (DP/MAS) NMR, ^{13}C Cross-Polarization/Total Suppression of Sidebands (CP/TOSS) and ^{13}C CP/TOSS Plus Dipolar Dephasing, ^{13}C Chemical-Shift-Anisotropy (CSA) Filter. Connectivities of different functional groups in hydrochars with ^{1}H–^{13}C Two-Dimensional Heteronuclear Correlation (2D HETCOR) NMR. Aromatic cluster sizes with ^{1}H–^{13}C Long-Range Recoupled H–C Dipolar Dephasing Experiments
Wiedner et al. [37]	Biochars (pyrolysis-Pyreg up to 850 °C, pyrolysis/gasification-BC up to 760 °C, gasification-AGT up to 1200 °C, gasification-CT up to 550 °C) and hydrochars (1st stage at 230 °C for at least 15 min and 2nd stage at 180 °C for at least 75 min; 170 °C for 90 min)	Wheat straw-AGT, wood chips-AGT, poplar-AGT, sorghum-AGT, olive residues-AGT, wood chips-CT, wood chips-BC, draff-Pyreg, miscanthus-Pyreg. Maize silage, leftover food, biogas digestate, grass greenery and sewage sludge for hydorchars	pH, EC, ash content, elemental composition (CHNO), ^{13}C NMR, SEM-EDS, black carbon content, PAHs content, polychlorinated dibenzodioxines (PCDDs) and polychlorinated dibenzofurans (PCDFs) content
Busch et al. [38]	Biochars (gasification-AGT up to 1200 °C and pyrolysis at 400–600 °C) and hydrochars (230 °C for 1 h and 180 °C for at least 4 h; 170 °C)	Olive residues-AGT, poplar wood chips-AGT, wheat straw-AGT, miscanthus-pyrolysis. Maize silage, food leftovers, biogas digestate grass and sewage eludge for hydrochars	Tradescantia genotoxicity assay, plant germination and growth tests and impact on soil pH
Busch and Glasser [39]	Biochar (pyrolysis-Pyreg), hydrochar (230 °C for 1 h and 180 °C for at least 4 h), co-composted biochar (1:1 w/w) and hydrochar (1:3 w/w) with raw biomass residues from vegetable waste from horticulture and landscaping, kept for 4 weeks in temperature range 55–75 °C)	Conifer wood bark residues for biochar and maize silage for hydrochar	Stability of co-composted hydrochar and biochar under field conditions in a temperate soil. TOC, total N content, pH, EC and black carbon analysis of biochars, hydrochars, compost and co-composted biochars and hydrochars before and after application in soil

2. Materials and Methods

Two different raw materials, pine wood chips (PW) and corn digestate (CD), were used for the production of biochar (pyrolysis) and hydrochar (HTC). PW was provided by Robeta Holz OHG (Milmersdorf, Germany) while CD was obtained from an anaerobic digester in Dorf Mecklenburg (Germany). The substrate used for mesophilic (39 °C) anaerobic digestion was 70% corn silage and 30% cow manure. The digestate was dried and stored on site. Due to storing conditions, the dry digestate contained a significant amount of calcium carbonate. The properties of both raw materials are shown in Table 2.

Table 2. Raw material, conversion process, experimental conditions and solid yields for biochar and hydrochar production. Ash content and elemental composition of pine wood chips (PW) and corn digestate (CD). Determination of ash content was done according to the DIN norm 51719. Elemental analysis was performed using a Vario EL elemental analyzer. Oxygen content was obtained by difference. The values are given in % mass, dry basis (%, db). * Maximum conversion temperature measured in the reference position, according to the description provided in the Section 1 of Supplementary Material.

Material	**Ash (%, db)**	**C (%, db)**	**H (%, db)**	**O (%, db)**	**N (%, db)**	
CD	19.6 ± 0.1	40.7 ± 0.7	5.5 ± 0.1	31.7 ± 0.8	2.4 ± 0.5	
PW	0.2 ± 0.0	49.4 ± 0.4	6.7 ± 0.1	43.7 ± 0.4	0.1 ± 0.0	
Sample	Raw material	Process	HTT * (°C)	Flow (NL min^{-1})	Char yield (%, db)	
PW400-20	Pine wood	Pyrolysis	400	20	30.01 ± 0.18	
PW400-40	Pine wood	Pyrolysis	400	40	25.83 ± 2.12	
PW600-20	Pine wood	Pyrolysis	600	20	24.94	
PW600-40	Pine wood	Pyrolysis	600	40	22.82 ± 0.49	
CD400-20	Corn digest.	Pyrolysis	400	20	50.89 ± 0.36	
CD400-40	Corn digest.	Pyrolysis	400	40	52.00 ± 0.21	
CD600-20	Corn digest.	Pyrolysis	600	20	49.76 ± 0.40	
CD600-40	Corn digest.	Pyrolysis	600	40	48.54 ± 1.08	
Sample	Raw material	Process	HTT (°C)	Time (min)	Wash. times	Char yield (%, db)
PW200-10	Pine wood	HTC	200	10	-	82.30 ± 0.35
PW200-360	Pine wood	HTC	200	360	-	75.68 ± 0.01
PW240-10	Pine wood	HTC	240	10	-	76.26 ± 0.07
PW240-360	Pine wood	HTC	240	360	-	59.09 ± 0.19
CD200-10-0	Corn digest.	HTC	200	10	0	83.49
CD200-10-6	Corn digest.	HTC	200	10	6	73.49
CD200-360-0	Corn digest.	HTC	200	360	0	74.38
CD200-360-6	Corn digest.	HTC	200	360	6	70.29
CD220-185-3	Corn digest.	HTC	220	185	3	64.57 ± 2.02
CD240-10-0	Corn digest.	HTC	240	10	0	70.82
CD240-10-6	Corn digest.	HTC	240	10	6	66.85
CD240-360-0	Corn digest.	HTC	240	360	0	62.06

CD and PW biochars were produced at the Technische Universität Berlin (Berlin, Germany), in a technical-scale fixed-bed reactor, with capacity for several kg of biomass. The setup used in these experiments has been presented elsewhere [40]. In these experiments, the influence of maximum pyrolysis temperature (400 and 600 °C) and residence time of the volatiles in contact with the solid bed (with inert gas flow rates of 20 and 40 NL min^{-1}) was investigated. Experiments were conducted in duplicates.

The hydrothermal carbonization experiments were carried out at the Leibniz Institute for Agricultural Engineering and Bioeconomy (Potsdam, Germany). Distilled water was added to the dry digestate in each experiment to achieve the desired solid content of 20% by mass. The experiments were conducted in a 1 L autoclave (Series 4520, stainless steel T 316, Parr Instruments, Moline, IL, USA) equipped with a temperature controller. The influence of maximum conversion temperature (200, 220 and 240 °C), time at this temperature (10, 185 and 360 min) and washing effect (0, 3 and 6 times with distilled water) on hydrochar properties was investigated.

Further details on biochar and hydrochar production conditions are given in Table 2 and in the Suplementary Material.

Analytical Methods

Biochars ash content determination was done following the DIN norm 51719. Hydrochars ash content was characterized according to the method described in Chapter 8.4 from the VDLUFA Methodenbuch Band III [41]. Validation of both methods for both raw materials showed that the results according to the DIN norm are within the standard deviation of the results from the VDLUFA method. For elemental analysis (CHNS), a Vario EL elemental analyzer (Elementar Analysensysteme GmbH, Lagenselbold, Germany) was used for hydrochars and biochars. Inorganic elemental analysis for hydrochars was performed in an ICP-OES (iCap 6300 Duo, from Thermo Scientific, Schwerte, Germany). Prior to the analysis, milled samples were digested according to the method exposed in Chapter 10.8 of the VDLUFA Methodenbuch Band III [41], using a microwave (ultraClave-IV high pressure microwave, from MWS Vertriebs GmbH, Leutkirch, Germany) with nitric acid 65% (260 °C, 140 bar, 2 h) and stored at room temperature. Biochar inorganic elemental characterization was also performed with an ICP-OES (Varian 720-ES, now Agilent Technologies, Inc., Santa Clara, CA, USA) after digestion in a microwave (Multiwave 3000, from Anton Paar, Graz, Austria) with nitric acid 65% (Rotipuran ® p.a., ISO, max 0.005 ppm Hg, Carl Roth GmbH + Co. Kg, Karlsruhe, Germany) and hydrogen peroxide 30% (Rotipuran ® p.a., ISO, stabilisiert, Carl Roth GmbH + Co. Kg, Karlsruhe, Germany).

The pH of biochars and hydrochars was measured in deionized water solution. The determination of oxygen-containing functional groups on the char surface was done applying the Boehm titration method [42]. The experimental procedure is based on the description by Goertzen et al. [43], including the sample pretreament proposed by Tsechansky and Graber [44]. Further details on this characterization method are given in the Section 2 of Supplementary Material.

The pore structure, including specific surface area, pore volume and pore size distribution, was characterized with gas adsorption, combining the measurement of N_2 and CO_2 adsorption isotherms at 77 K and 273 K respectively. The pretreatment of the samples, prior to adsorption measurements, included milling and degassing in vacuum at 150 °C during 6 h, with the objective of cleaning the surfaces from other adsorbed species and reducing transport limitations (milling). For both degassing and adsorption/desorption measurements the gas sorption system Nova 2200, provided by Quantachrome Instruments (Boynton Beach, FL, USA), was used. Several methods were applied to the isotherms in order to derive pore surface areas and volumes, all of them included in the NovaWin software (Version 11.04, also from Quantachrome Instruments). The methods applied to the N_2 adsorption/desorption isotherms included: the BET method [45] to meaure the total specific surface area; the BJH method [46] to characterize the specific surface area and volume of pores bigger than ≈3 nm; and the density functional theory (DFT) [47] method, in particular, the quenched solid density functional theory (QSDFT) method, considering slit/cylindrical pores (Quantachrome Instruments). With the QSDFT method, the specific surface area and volume of micropores and mesopores up to ≈34 nm were characterized. The total pore volume was determined from the volume of N_2 adsorbed at a relative pressure $P/P_0 \approx 1$, assuming that at this point the pores are filled with liquid N_2. For CO_2 adsorption, the non local density functional theory (NLDFT) method (Quantachrome Instruments) was applied to determine the specific surface area and volume due to micropores up to ≈1.5 nm.

Biochar thermal stability was analyzed by thermogravimetric analysis (TGA 1, STARe system, from Mettler Toledo, Columbus, OH, USA) with a heating rate of 5 °C min^{-1}, in synthetic air (20.5% O_2, 200 mL min^{-1} air flow) and up to a temperature of 600 °C. Initial mass below 5 mg was used to guarantee kinetic regime and avoid self-heating due to the exothermicity of the oxidation reactions. Conversion rate of biochar oxidation is defined here as the change of conversion (α) over time ($\frac{d\alpha}{dt}$). Conversion (α) is defined as $1 - (m_o - m)/(m_o - m_f)$, where m is the biochar mass at each time step, m_o is the initial biochar mass and m_f is the mass of the combustion product at 600 °C, i.e., ash.

Plant available ammonium (NH_4^+) and nitrate (NO_3^-) were determined according to the DIN 19746:2005-06 (extraction of the samples with 0.0125 mol L^{-1} of $CaCl_2$ in distilled water). Plant available phosphate (PO_4^{3-}) and potassium (K^+) were determined according to VDLUFA Methodenbuch Band I [48], Chapter 6.2.1.1 (extraction with a solution of 0.02 mol L^{-1} of calcium lactate and 0.02 mol L^{-1} hydrochloric acid in distilled water). The analysis of the extracts was conducted by IC-CD (ICS 1000, from DIONEX). Anions were analyzed with an IonPac AS9-HC 4 × 250 mm column from DIONEX (chromatographic conditions: 9 mmol Na_2CO_3, 1.2 mL min^{-1}, 160 bar) and cations with an IonPac CS 16 5 × 250 mm column from DIONEX (chromatographic conditions: 30 mmol methanesulfonic acid (MSA), 1.0 mL min^{-1}, 80 bar, 40 °C).

The method applied for characterization of the 16 USEPA (United States Environmental Protection Agency) PAHs has been developed by Fabbri et al. [49], with the difference that in the present study a standard solution of deuterated 16 PAHs (PAH-Mix 9 deuterated, 10 mg L^{-1}, Dr. Ehrenstorfer, Augsburg, Germany) was used, instead of 3 deuterated PAHs as in [49]. Briefly, the biochar samples, spiked with 0.1 mL of a 5 mg L^{-1} solution of the above deuterated 16 PAHs solution, were Soxhlet extracted with an acetone (CHROMASOLV, for HPLC, ≥99.9%, Sigma–Aldrich, St. Louis, MO, USA)/cyclohexane (ACS reagent, ≥ 99.5%, Sigma–Aldrich, St. Louis, MO, USA) (1:1, *v*/*v*) solvent mixture for 36 h and then the PAHs were analyzed in an Agilent HP 6850 gas chromatograph (GC) coupled to an Agilent HP 5975 quadrupole mass spectrometer (MS) (Agilent Technologies, Inc., Santa Clara, CA, USA); GC-MS conditions were those detailed in [49].

Biochar wettability measurements were performed according to the method described by Ojeda et al. [50]. Briefly, a glass tube 6 cm high with 0.9 cm of internal diameter was filled with the different biochar samples up to a height of 3 cm. Then the tube was attached to a high precision scale (DCAT, dynamic contact angle measuring instrument, DataPhysics©, Germany). Below the tube, a glass filled with distilled water or n-hexane (AnalaR NORMAPUR –for synthesis– ≥95%) was placed and carefully risen until touching the bottom part of the tube. Distilled water/n-hexane capillary absorption was measured by registering the weight increase in the biochar column during 200 s.

3. Results and Discussion

3.1. Primary Characterization: Yields, Elemental and Proximate Analysis

In Table 2 biochars and hydrochars yields are presented. Hydrochars show significantly higher char yields than biochars, consistent with the lower conversion temperatures and the higher pressures. For biochars, the lower the conversion temperature the higher the char yield. CD biochars also present higher yields than PW biochars, due to the significantly higher inorganic species content, which remain in the solid product after pyrolysis. Besides, a higher N_2 flow rate during pyrolysis generally reduces the char yield, due to a reduction in the residence time of the volatiles in the bed, minimizing secondary reactions and formation of secondary char [12]. In the case of hydrochars, the solid yields for both raw materials are similar. Besides, both conversion temperature and retention time at the conversion temperature play an important role. Noteworthy to mention in the case of hydrochars is the impact of washing. With the same conversion temperature and retention time, washing the hydrochar after production can reduce up to 10% the solid yield. This indicates that a significant part of the solid is actually condensed volatiles and water soluble inorganic species.

In Figure 1 (left), the Van Krevelen diagram, i.e., the representation of H/C molar ratio versus O/C molar ratio is presented for biochars and hydrochars. This diagram is often used to illustrate the degree of maturity and aromaticity of chars [51]. Results in Figure 1 show that hydrochar and biochar chemical composition depends on the conversion conditions, but also on the initial feedstock composition, having potentially a significant impact on final char chemical properties. This is illustrated with the results of CD biochars/hydrochars versus those for PW biochars/hydrochars. For the same O/C molar ratio, the H/C molar ratio of CD biochars is lower than for PW biochars. Looking at the relation of these molar ratios with the volatiles content (% mass, dry ash free), it is observed that while biochar O/C molar ratio follows a linear trend with respect to the volatiles content, the behavior of H/C ratio seems only linear for PW biochars, while very scattered for CD biochars.

As it has been introduced in Section 2, corn digestate contains calcium carbonates, mainly due to storing conditions. The inorganic C content of CD biochars, due to carbonates, is approximately 4–5%, as determined by Rombolà et al. [52]. The presence of these carbonates could explain, to some extent, the higher volatiles content of CD biochars in comparison with PW biochars, since at the conversion temperatures used in this study (400 and 600 °C) carbonates are stable and therefore remain in the biochar. However, this could not explain the lower content in hydrogen for CD biochars. Besides, the elemental composition of CD presented in Table 2 is similar to the one reported by Mumme et al. [53] for maize silage digestate. This suggests different reaction pathways for low and high inorganic matter content biochars, with a potential enhancement of aromatization for high inorganic matter content biochars. Li et al. [54] also reported lower H/C ratios for biochar produced from pyrolysis of rice husk, blended with $CaCO_3$ prior pyrolysis, than for unmodified biochars, which they correlated with an increase in the carbon aromaticity degree. The potential formation of oxides or other metal composites on the biochar surface, associated to the high content of inorganic matter, could also play a role [55].

With respect to hydrochars, CD hydrochars present in general higher H/C ratios and lower O/C ratios than PW hydrochars, in some cases even lower than CD biochars. This indicates different reaction mechanisms for both materials. The higher H/C ratios of CD hydrochars suggests that decarboxylation reactions are favored over dehydration reactions [53]. In the case of PW hydrochars, dehydration reactions seem to be more significant in comparison to CD hydrochars, while the influence of decarboxylation reactions is lower, except for the highest conversion temperature and highest retention time (240 °C – 360 min), where both are relevant. This is further supported by the composition of the producer gas (collected during the HTC experiments in gas bags and analyzed with a SSM6000 analyzer from Pronova, Germany), with a concentration of CO_2 increasing from around 50% vol. to approximately 80% vol. for the highest conversion degree. It is also important to point out that retention time at the conversion temperature is as significant as the conversion temperature itself. With respect to CD hydrochars, CO_2 increases from approximately 58% vol. from the mildest conditions to around 75% for the most severe conditions. In this case, a significant emission of CH_4 (2.5% vol.) was also registered. Alkaline conditions during HTC enhance the formation of carboxylic acids, reducing therefore the O/C ratio of the hydrochar [56]. In the present study, although the pH of both solid and liquid products are acid, they are higher for CD hydrochars than for PW hydrochars, as shown in Section 3.2. Similar composition for digestate hydrochars has been also shown by Mumme et al. [53], who highlighted that this could be due to the decarboxylation reactions. Liu et al. [28], who compared a hydrochar produced at 300 °C with a biochar produced at 700 °C using pine wood, reported similar H/C and O/C ratios for their biochar as for the PW biochars produced at 600 °C in the present study. The values for the hydrochar were slightly higher in comparison to PW hydrochars produced at 240 °C during 360 min in the present study. Besides, for similar hydrochar H/C ratio, the hydrochar O/C ratio is lower in the present study than in [28]. This could be related to the high amount of ash reported by Liu et al. [28].

According to the guidelines given by the European Biochar Certificate (EBC) [1] and the International Biochar Initiative (IBI) Standards [2] on H/C and O/C ratios, the biochars presented in this Section could be considered as certified biochars. With respect to hydrochars, it is shown that it is also possible to produce hydrochars able to fulfill those requirements, with a conversion temperature of at least 240 °C and a retention time of 360 min, but only with starting HTC conditions enhancing both dehydration and decarboxylation reactions (as it is the case for PW), not only decarboxylation reactions (as in the case of CD).

Inorganic elemental characterization is shown in Table 4 and in the Supplementary Material (Table S1). It is observed that the elemental inorganic composition of CD hydrochars and biochars is much higher than the one for PW hydrochars and biochars, in good agreement with their high ash content.

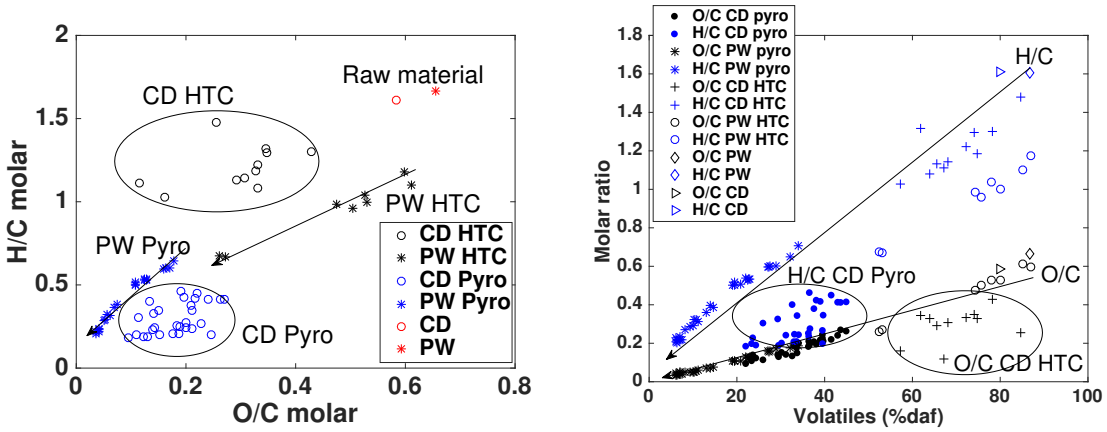

Figure 1. Left: Van Krevelen diagram, i.e., H/C molar ratio versus O/C molar ratio of PW and CD biochars and hydrochars. **Right**: H/C and O/C molar ratios versus volatiles content (% mass, daf) for PW and CD biochars and hydrochars.

3.2. pH and Surface Functional Groups

It has been reported in literature that pH may be dependent on both, the surface chemistry and the ash content [22,23,57,58]. These both influences are further confirmed in the present study. In Figure 2a,b the variation of pH with ash content is presented. Biochars with higher ash content show also higher pH. However, the strongest correlations for biochars are not between pH and the ash content, but between pH and H/C and O/C molar ratios. Specially remarkable is the correlation between pH of CD biochars and H/C molar ratio ($r = -0.95$, shown in Figure 2c, being r the Pearson correlation coefficient), when considering that the latter shows such scattered behavior in Figure 1. It must be also taken into account that CD contains calcium carbonate due to storing conditions, which has a high liming effect. However, the correlation between CD biochars ash content and pH is significantly worse than between pH and H/C. With respect to PW biochars, pH presents also stronger relations with H/C and O/C molar ratios ($r = -0.91$ and $r = -0.89$ respectively, shown in Figure 2d,f) than with ash content, being this correlation similar in both cases.

Therefore, with respect to biochars pH, it can be concluded that despite the fact that ash content has an influence on the pH value, a better correlation exists between the pH value and H/C and O/C ratios. In the case of CD biochars, the relation between pH and H/C ratio is strongly linear.

For hydrochars the behavior is slightly different. Figure 2a shows that pH of CD hydrochars has a stronger correlation with ash content ($r = 0.88$) than with H/C (Figure 2c) or O/C ratios (Figure 2e). Despite the fact that the slope of the linear fitting for pH-ash in Figure 2a for CD hydrochars is lower than those for pH-H/C for CD and PW biochars in Figure 2c,d respectively, the correlation is still much better for pH-ash than for pH-H/C or pH-O/C. This indicates that the pH in CD hydrochars is

mainly correlated to ash content, although with a weaker dependency than PW and CD biochars pH with H/C ratio. PW hydrochars show similar relations with H/C and O/C molar ratios.

In Figure 3, information about the acidic functional groups present on the chars surface is given, in particular, for carboxylic, phenolic and lactonic groups. In Figure 3a the total acidic functional groups (carboxylic, lactonic and phenolic) and the carboxylic functional goups with respect to the organic fraction of the chars (mmol g_{org}^{-1}, db) are plotted versus the O/C molar ratio for PW600-20, PW400-20, PW600-40, PW400-40, CD600-20, CD400-20, PW240-10. For biochars, independently of the inorganic matter content, a good correlation (r = 0.80) is observed between total acidic groups and O/C ratio. Hydrochar PW240-10 presents a high O/C molar ratio which does not correlate well with the total acidic functional groups, according to the biochars behavior. This may indicate that still a significant amount of oxygen is embedded in the hydrochar skeleton, which is in good agreement with the structure of hydrochar formed mainly by alkyl moieties reported by Cao et al. [36]. In Figure 3b the total acidic groups and the carboxylic goups (with respect to the organic fraction of the chars) are plotted versus H/C molar ratio. No good correlations are observed. However, in Figure 3c a quite strong linear correlation (r = 0.84) is present between the total surface acidic groups with respect to the total char mass (mmol g^{-1}, db) and the H/C molar ratio, independently of the inorganic matter content and the conversion process. Figure 3d shows the comparison of these groups with pH. A relation between the increase in pH and the decrease in total acidity of the biochar surface is observed.

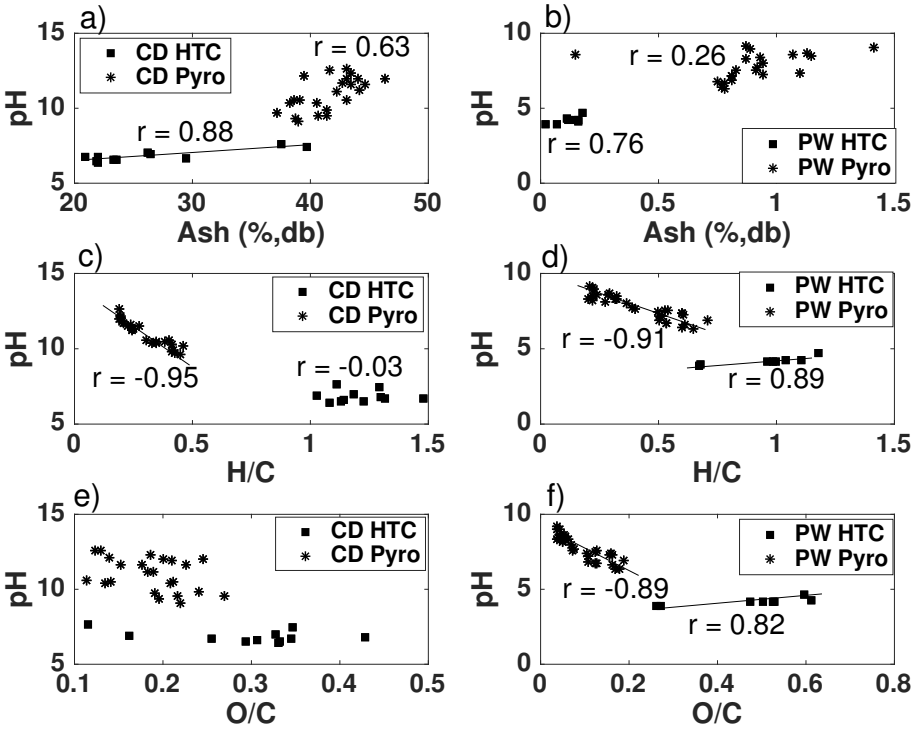

Figure 2. pH versus ash (% mass, db) in (**a**,**b**), H/C molar ratio in (**c**,**d**) and O/C molar ratio in (**e**,**f**) for CD (left) and PW (right) biochars and hydrochars. The strength of the correlations is indicated with the Pearson correlation coefficient (r).

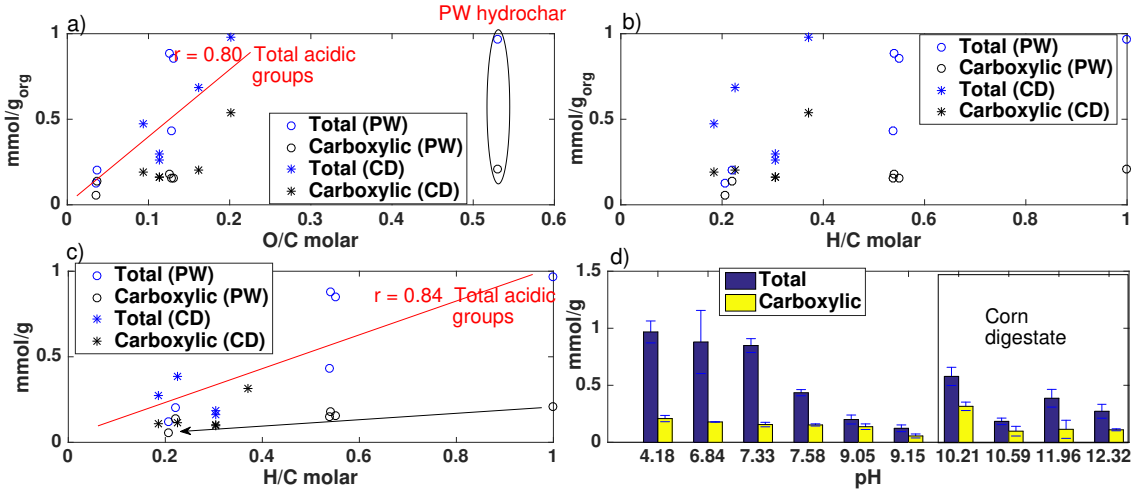

Figure 3. Surface oxygen-containing functional groups of the biochars determined with the Boehm titration method. (**a**,**b**) show the amount of functional groups with respect to the mass of the chars organic fraction versus the O/C and H/C molar ratios; (**c**) shows the amount of functional groups with respect to the total chars mass versus the H/C molar ratio; (**d**) shows the amount of functional groups versus the pH.

3.3. Porosity Characterization

In Figure 4, the evolution of the total specific surface area (BET method using N_2 adsorption) is plotted versus the biochars/hydrochars volatiles content (% mass, daf). In general, the lower the volatiles content, the higher the specific surface area (SSA). However, for CD biochars different BET SSA behaviors are observed for similar volatiles content. The highest SSA values correspond to biochar produced at 600 °C with a N_2 sweeping flow rate of 40 NL min^{-1}. In Figure 4b the SSA evolution is plotted versus the H/C molar ratio. The decrease of H/C molar ratio is indicative of the formation of structures containing unsaturated carbon such as aromatic rings [59], and therefore, represents the increase in aromaticity with charring degree, as reported in [25]. It is possible to observe that the behavior of CD biochars differs significantly from the one of PW biochars. Taking into account that CD biochars have around 40% ash content, the SSA would be higher as function of the organic fraction, but it would be still lower than for PW biochars. This may be a consequence of two possible phenomena: (a) porosity development is different for materials with high inorganic content and (b) potential filling or access blocking of micropores by the inorganic species [60,61], which could explain the lower SSA value despite the lower H/C molar ratio in CD biochars.

In order to further characterize the porous structure, in Figure 5 the pore size distribution according to pore surface area (left) and pore volume (right) is presented, characterized with the methods introduced in Section "Analytical Methods". SSA and volume from CO_2 adsorption are also shown in Figure 5. With CO_2 adsorption, micropores up to 1.5 nm in pore width are characterized. Despite this, the SSA area measured with CO_2 adsorption is higher than the total SSA (up to 100–200 nm in pore width, depending on the sample porous structure) measured with N_2 adsorption. This indicates that the samples have a microporous structure which cannot be completely characterized by N_2 adsorption, mostly due to diffusion limitations, consequence of the low temperature measurements in N_2 adsorption.

The CO_2 SSA is around 25% higher than the N_2 SSA for PW biochars produced at 600 °C, with inert gas flow rates of 20 and 40 NL min^{-1}. However, the CO_2 SSA for CD biochars produced in the same conditions is 90% and 80% higher respectively. This indicates that the diffusion limitations are stronger in CD biochars, in good agreement with the previous explanation for the low specific surface of high inorganic content biochar. That is to say, the inorganic species may provoke partial blocking or constriction of the porous structure, limiting the access of N_2 to micropores but not of CO_2.

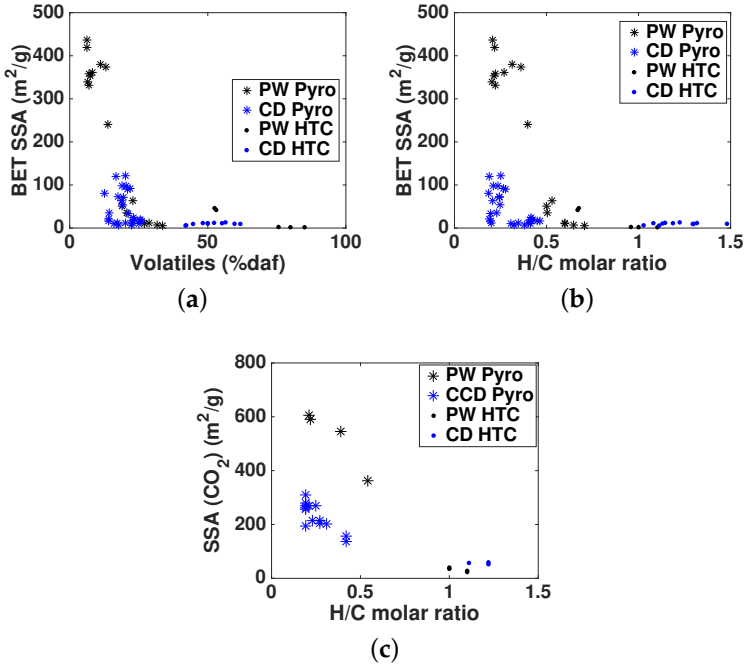

Figure 4. (**a**): Total specific surface area (SSA) determined with the BET method (N_2 adsorption) versus the volatiles content (% mass, daf) for PW and CD biochars and hydrochars; (**b**): SSA determined with the BET method (N_2 adsorption) versus H/C molar ratio for PW and CD biochars and hydrochars; (**c**): SSA determined with CO_2 adsorption applying the NLDFT method versus H/C molar ratio for PW and CD biochars and hydrochars.

With respect to the pore volume, higher N_2 pore volume than CO_2 pore volume is measured for PW biochars produced at 600 °C. This is due to the smaller size of pores characterized by CO_2 adsorption. Noteworthy to mention is the fact that higher N_2 sweeping flow during the pyrolysis process leads to higher SSA and pore volume in the biochar. For PW biochars the effect is clearer when looking at the pore volume distribution. This is also stronger for biochars produced at 400 °C than for biochars produced at 600 °C. For CD biochars the difference for biochars produced at 600 °C is already very significant, as introduced in Figure 4. This shows that higher flow rates lead to a more open porous structure, due potentially to a combination of higher removal of volatiles (more significant for biochars produced at 400 °C) and inorganic species (present in CD biochars), together with lower extent of intraparticle heterogeneous secondary reactions, leading to the formation of secondary char.

Interestingly, while the major contribution to pores in PW biochars comes from micropores (observed in the CO_2 adsorption results), in CD biochars the contribution of mesopores is also significant. Therefore, inorganics in CD biochars would not only reduce the presence of micropores through potential blocking, but could also enhance the development of mesopores.

Comparing the porous structure of hydrochars with the one of biochars, the former follows quite a different behavior. According to Figure 4, hydrochars present low SSA, in good agreement with the high volatiles content and high H/C molar ratio. This suggests low charring and aromatization degree in comparison with biochars. However, in Figure 5, results for hydrochars pore size distribution, according to volume (bottom right), show that the volume of these samples is in many cases higher than the one of biochars. Contribution of micropore volume to the total pore volume of hydrochars is low. Therefore, it can be concluded that porosity (pore volume) in hydrochars is mainly due to meso- and macropores. Comparing PW hydrochars and CD hydrochars produced at 240 °C, with a retention time at maximum conversion temperature of 360 min, it is possible to see that PW hydrochars present significantly higher SSA and volume. This could be attributed to the high inorganic matter content

of CD hydrochars. However, PW hydrochars produced at 240 °C during 10 min or at 200 °C during 360 and/or 10 min show lower SSA and volume than CD hydrochars produced at 240 °C and 200 °C during 360 min. Comparing the behavior of CD hydrochars produced at 240 °C and 200 °C during 360 min, the SSA and pore volume of the latter are higher despite the lower conversion temperatures. This is due to the washing of the hydrochar produced at 200 °C during 360 min. This washing removes inorganics and volatiles partially blocking the pores, which leads to an underestimation of the porous structure with N_2 adsorption, as previously introduced for biochars. However, CO_2 adsorption results show similar values of microporosity for both cases, indicating that this pore blocking does not affect CO_2 adsorption.

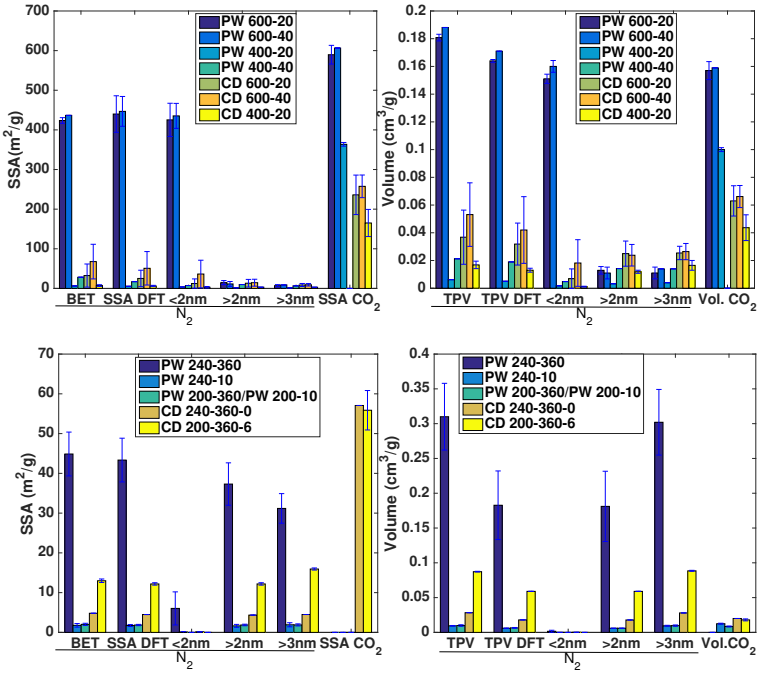

Figure 5. Pore size distribution (PSD) of PW and CD biochars (**top**) and hydrochars (**bottom**). **Top left**: SSA distribution with pore size for biochars according to the BET method (for total specific surface area), quenched solid density functional theory (QSDFT, for total specific surface area, surface area due to pores < 2 nm and pores 2 nm < pore size < 34 nm) method, and BJH method (surface area due to pores > 3 nm). Total specific surface area for pores < 1.5 nm determined with CO_2 adsorption. **Top right**: Volume distribution with pore size for biochars. **Bottom left**: SSA distribution with pore size for hydrochars according to the aforementioned methods. **Bottom right**: Volume distribution with pore size for hydrochars. CO_2 adsorption was not measured for samples PW400-40 and PW240-360.

3.4. Thermal Stability

Oxidation behavior of biochar in the presence of synthetic air has been performed in a thermogravimetric analyzer (TGA) to assess biochar stability to oxidation [62,63].

In Figure 6, the conversion rate under oxidation conditions is plotted versus the temperature for hydrochars (top) and biochars (bottom). The higher the temperature correspondent to the peak of the conversion rate, the lower the reactivity, and therefore, the higher the stability to oxidation.

For most hydrochars, except the ones produced under the highest severity (240 °C, 360 min retention time), a first peak in the conversion rate is observed at temperatures slightly above 300 °C, consistent with further oxidative pyrolysis of the sample [64]. The second peak at higher temperatures is related to char oxidation. For PW hydrochars, these oxidation peaks take place at significantly higher temperatures than for CD hydrochars. At the same time, water washing of the hydrochars after production seems to also affect their oxidation behavior. Those not being washed experience an

earlier second oxidation peak. For biochars, the higher the conversion temperature, the higher the temperature correspondent to the maximum of the oxidation peak. For hydrochars, residence time at the maximum conversion temperature and post-washing, as previously introduced, also play a significant role.

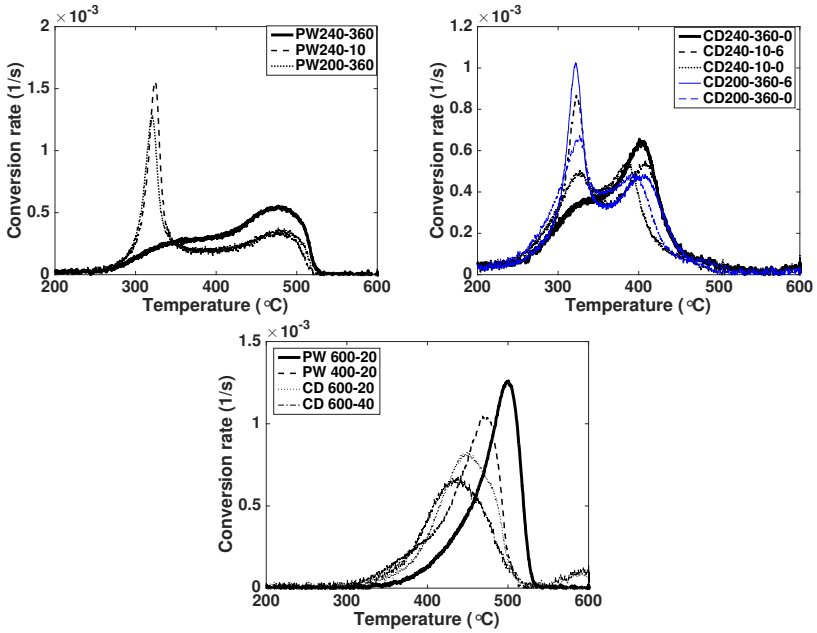

Figure 6. Conversion rate of char oxidation for PW hydrochars (**top left**), CD hydrochars (**top right**), PW and CD biochars (**bottom**).

The initial feedstock seems to have a stronger influence on the thermal stability (based on the shape and peak position of the char oxidation curve) than the conversion process conditions. It is known from literature [12] that char reactivity (in oxidation and gasification conditions) depends on the char structure at molecular level, the inorganic matter in the carbon skeleton, specially alkali and alkaline earth metals (AAEM), and the concentration and type of functional groups in the carbon skeleton. Consequently, the high inorganic content of CD biochars, including AAEM, could act as catalyst in biochar oxidation. This is also consistent with the washing of hydrochars, since with washing, inorganic species can be removed from the hydrochar surface. Harvey et al. [65] showed a similar behaviour with biochars (produced in [66]) from loblolly pine and cord grass, i.e., lower $R_{50,biochar}$ for biochars with high inorganic content (up to 30% ash content for cord grass). However, regardless of the inorganic content, they attributed the differences in biochar thermal stability to the extent of carbonization/aromatization. Therefore, samples with similar H/C and O/C ratios can have different recalcitrance depending on the rearragement of these atoms in the biochar structure [65].

Correlation between the thermal stability and the biogeochemical stability of soil organic matter has been proposed by Plante et al. [67]. Harvey et al. [65] reported also a strong negative exponential-type relationship between biochar degradabitlity (based on the amount of carbon mineralized after 1 year of incubation [68]) and the thermal recalcitrance $R_{50,biochar}$, defined according to Equation (1). $T_{50,biochar}$ is the temperature correspondent to 50% conversion of biochar (i.e., 50% of the total mass loss due to oxidation/volatilization) and $T_{50,graphite}$ is analog for graphite. In Table 3, the $R_{50,biochar}$ values for several biochars and hydrochars are shown, considering $T_{50,graphite}$ = 844 °C [62]. If a $T_{50,graphite}$ = 886 °C is used, as measured by Harvey et al. [65], slightly lower $R_{50,biochar}$ values are registered (values between parentheses in Table 3).

$$R_{50,biochar} = \frac{T_{50,biochar}}{T_{50,graphite}} \quad (1)$$

Table 3. $R_{50,biochar}$, C (% mass, daf), H/C and O/C molar ratios for biochar and hydrochar samples. The $R_{50,biochar}$ values are calculated considering a $T_{50,graphite}$ = 844 °C [62]. The $R_{50,biochar}$ values between parentheses correspond to a $T_{50,graphite}$ = 886 °C [65].

	$R_{50,biochar}$	C (% mass, daf)	H/C (molar)	O/C (molar)
PW200-360	0.43 (0.41)	56.94	0.96	0.50
PW240-10	0.41(0.39)	55.77	1.00	0.53
PW240-360	0.51 (0.48)	70.33	0.67	0.27
CD200-360-0	0.41 (0.39)	62.93	1.19	0.33
CD200-360-6	0.41 (0.39)	62.86	1.22	0.33
CD240-10-0	0.43 (0.41)	61.69	1.29	0.35
CD240-10-6	0.42 (0.40)	61.77	1.32	0.35
CD240-360-0	0.45 (0.43)	76.35	1.11	0.12
PW400-20	0.53 (0.50)	82.10	0.54	0.13
PW600-20	0.57 (0.54)	93.49	0.22	0.04
CD600-20	0.52 (0.50)	84.62	0.18	0.09
CD600-40	0.52 (0.50)	81.99	0.19	0.13

According to a biochar classification proposed by Harvey et al. [65], all analyzed biochars are Class B biochars ($0.50 \leq R_{50,biochar} < 0.70$), with intermediate C sequestration potential, while the rest are Class C biochars ($R_{50,biochar} < 0.50$), which indicate that those chars have carbon sequestration potential comparable to uncharred biomass. The PW240-360 hydrochar could belong to both classes, depending on the considered $T_{50,graphite}$.

3.5. Nutrients

The total content of macronutrients, such as Ca, Mg, N, P and K, is presented in Table 4 for PW and CD biochars and hydrochars. These values are compared with the available nutrient content in the form of NH_4^+, NO_3^-, PO_4^{3-} and K^+.

Due to methodical issues, the values of hydrochars nutrient availability, determined from the solid fraction, cannot be directly compared with those for biochars. A significant fraction of the investigated species is solved in the liquid phase during HTC, which might still be present upon drying of the hydrochar. This fact leads to measured nutrient availability in the hydrochar that is not a representative hydrochar characteristic [69]. Instead, the behavior of the nutrients under consideration is investigated via measurements of the liquid phase for the case of hydrochars. Therefore, for hydrochars, the content of Ca, Mg, K and P in the solid and in the liquid phase are presented.

It is observed that the main factor affecting nutrient content in the final product is the feedstock, since both present very different composition, with higher inorganic species and N content in CD. It is obvious that PW has negligible potential for direct nutrient value from this point of view. Such direct nutrient value is high for CD due to high amount of available N, P, and K (see Table 4). In the case of CD it becomes important to investigate how the total nutrient content and their availability changes with the conversion process. PW results are also presented as comparison.

The ratio C/N can be used as a possible indicator for nitrogen mineralization or immobilization, taking C/N < 20 as predictor for nitrogen mineralization and C/N > 30 as indicator of initial net nitrogen immobilization [37,70]. For PW biochars the molar C/N ratio is very high, with values above 500, which could potentially lead to a high degree of N immobilization once applied to soil, as previously explained. This is due to the low content of nitrogen in the initial feedstock, which would

still decrease during the conversion process due to nitrogen volatilization, leaving negligible amount of available N-species in the biochar [17]. In the case of CD, the initial nitrogen content in feedstock is significantly higher, leading to C/N ratios between 20 and 30, which would indicate possibility of mineralization or higher availability for plants once applied to soil [37]. However, the amount of available N-species for CD biochars is negligible, similar to PW biochars. It must be taken into account that the C/N ratios for hydrochars are indicative, due to the aforementioned methodical issues.

With respect to P and K, PW biochars present higher nutrient availability (PO_4^{3-} and K^+) in comparison to the raw feedstock. This may be explained by accumulation of these elements due to release of volatile organic matter during pyrolysis for the case of K^+ availability, which also shows a highly significant ($p < 0.001$) dependency on pyrolysis temperature. PO_4^{3-} availability does not seem to be dependent on temperature but rather on N_2 gas flow at 600 °C ($p < 0.05$). In contrast to PW, CD biochars PO_4^{3-} availability is reduced in comparison to the feedstock. Also, there is the same significant ($p < 0.05$) dependency on N_2 gas flow at 600 °C pyrolysis temperature. The observed reduction in K^+ availability for the case of CD is not significant due to the high uncertainty associated with the results (which stems from the high heterogeneity of the feedstock).

A reduction in the availability of PO_4^{3-} has been reported elsewhere, but different to the observed results in this study, a dependency on pyrolysis temperature has been reported [16,17]. Instead, in this study an increase in N_2 flow leads to a significant increase in PO_4^{3-} availability at high pyrolysis temperature. This hints to the hypothesis that P is somehow included in carbonaceous solids formed upon recondensation of primary pyrolysis vapors because it has been shown that biochar extractable P is primarily orthophosphate at pyrolysis temperatures > 350 °C [16]. More detailed studies are required to understand this phenomenon. Finally it has to be concluded that pyrolysis leads to a significant loss of plant available nutrient species, specifically NH_4^+, NO_3^-, and PO_4^{3-}, which has to be considered when nutrient rich feedstock is being used.

In contrast to the observations from pyrolysis experiments, HTC of PW does lead to a significant increase of N, P, and K availability (as defined by the analytical method applied here). Twice to ten times the amount of nutrients are recovered in the process water of HTC as compared to the leachate after extracting with $CaCl_2$ or double lactate (see Table 4, note that at least four times as much process water is present after HTC as dry solid input). These leached nutrients are lost to the hydrochar, but can be potentially re-used together with the process water. Different to pyrolysis, nitrogen compounds are not lost during the conversion process [69,71]. HTC of nutrient rich CD leads to different observations: the same amount of available nutrients of the feedstock are recovered in the process water for the case of NH_4^+ and K^+, but there is a significant reduction of NO_3^- and PO_4^{3-}. This is likely due to the precipitation of salts, leading to a recovery of these nutrients with the solids [72]. Indeed, the observed high amount of extractable PO_4^{3-} on the hydrochar (data not shown) cannot be explained by solved PO_4^{3-} in the hydrochars moisture content, i.e., that a significant amount of solid PO_4^{3-} precipitates during the reaction. It is also noted that the P contained in the liquid phase is almost exclusively detected as PO_4^{3-} whereas only a fraction of the hydrochars P is extractable by the applied methods (10–30%). The recovery of nutrients in the process water allows for a decoupling of fertilizing and soil amendment with the potential to flexibly combine these two in a designed hydrochar product. There is only little influence of the applied HTC process conditions on these findings. For the case of PW, more severe carbonization leads to a significant but small reduction of NH_4^+ and PO_4^{3-} in the liquid phase ($p < 0.05$). This might be due to an increase in adsorption capacity of the produced hydrochar or increased precipitation of these species. For the case of CD, this decrease with reaction severity is only observed for NO_3^- and PO_4^{3-} ($p < 0.05$). These results are in contrast to observations from other HTC experiments, which reported an increase of NH_4^+ in the liquid phase with reaction temperature or no significant change at all [69,72]. These contradicting results can be possibly explained with the varying nutrient concentrations used in the different experiments.

Table 4. Total content of N, Mg, Ca, P and K, as well as available N, P and K (mean ± standard deviation). The inorganic species content is given for the solid phase (sol) in biochars and for the solid (sol) and liquid phase (liq) in hydrochars. [a] determined by biochar extraction. [b] measured in the liquid phase of the hydrothermal carbonization experiments. n.d.: not detected. * The ratio C/N is molar ratio.

	C/N_{sol} *	N_{sol} (db)	Mg_{sol} (db)	Ca_{sol} (db)	P_{sol} (db)	K_{sol} (db)	Mg_{liq}	Ca_{liq}	P_{liq}	NH_4^+	NO_3^-	PO_4^{3-}	K^+
	-	%	mg/kg	mg/kg	mg/kg	mg/kg	-	-	-	mg/kg [a]	mg/kg [a]	mg/kg [a]	mg/kg [a]
PW	912.7	0.1	178.1 ± 38.7	894.5 ± 305.7	-	322.1 ± 81.6	-	-	-	2.3	0.9	13	230
CD	20.1	2.4	-	-	13,900 ± 440	9600 ± 360	-	-	-	1200 ± 110	1800 ± 130	1800 ± 160	6100 ± 350
PW400-20	550.9 ± 57.9	0.2 ± 0.0	-	-	-	-	-	-	-	n.d.	0.9	27 ± 9	300 ± 30
PW400-40	729.2 ± 54.2	0.1 ± 0.0	-	-	-	-	-	-	-	n.d.	n.d.	37 ± 2	370 ± 60
PW600-20	634.1 ± 106.8	0.2 ± 0.0	-	-	-	-	-	-	-	0.9 ± 0.2	n.d.	16 ± 2	900 ± 40
PW600-40	694.3 ± 91.3	0.2 ± 0.0	-	-	-	-	-	-	-	0.4 ± 0.1	0.6	43 ± 6	750 ± 40
CD400-20	22.6 ± 3.5	2.4 ± 0.4	20,568.0 ± 2233.3	139,051.2 ± 23,155.2	26,458.0 ± 2163.8	11,882.6 ± 1303.1	-	-	-	1.2 ± 0.5	n.d.	1360 ± 110	4610 ± 1680
CD400-40	22.4 ± 0.2	2.3 ± 0.1	22,608.3 ± 3140.2	154,160.6 ± 25,380.1	30,319.7 ± 3287.0	13,184.2 ± 1594.7	-	-	-	2.6	n.d.	1650	7460
CD600-20	29.4 ± 1.5	1.8 ± 0.1	21,796.2 ± 1781.4	135,010.5 ± 15,103.8	27,975.3 ± 2270.6	12,410.9 ± 1441.5	-	-	-	1.4 ± 0.4	11	960 ± 130	7890 ± 1580
CD600-40	29.6 ± 1.4	1.7 ± 0.1	22,150.4 ± 2930.0	156,042.0 ± 13,715.9	29,015.1 ± 3091.5	12,601.1 ± 1442.5	-	-	-	1.3 ± 0.1	n.d.	1510 ± 50	8210 ± 1410
	[-]	%	mg/kg	mg/kg	mg/kg	mg/kg	mg/kg	mg/kg	mg/kg	mg/kg [b]	mg/kg [b]	mg/kg [b]	mg/kg [b]
PW200-10	522.8 ± 80.7	0.1 ± 0.0	95.8 ± 9.8	733.1 ± 54.3	61.5 ± 4.2	213.1 ± 19.5	60.0 ± 8.8	126.7 ± 38.3	31.7 ± 9.4	5.1 ± 0.2	5.3 ± 0.5	24.2 ± 7.5	124 ± 20
PW200-360	841.7 ± 68.6	0.1 ± 0.0	99.3 ± 14.8	446.6 ± 14.1	78.7 ± 31.3	255.4 ± 9.6	48.2 ± 8.7	145.1 ± 10.7	16.0 ± 1.1	1.1 ± 0.1	5.5 ± 1.9	11.4 ± 1.1	112 ± 2
PW240-10	616.1 ± 248.0	0.1 ± 0.1	72.0 ± 0.1	500.1 ± 4.0	48.9 ± 3.0	183.4 ± 9.3	42.8 ± 0.4	135.6 ± 1.2	22.3 ± 0.1	2.1 ± 0.2	5.9 ± 0.0	17.4 ± 0.6	115 ± 3
PW240-360	1802.3 ± 1351.3	0.1 ± 0.1	118.4 ± 4.6	624.8 ± 16.7	71.2 ± 1.3	336.0 ± 31.1	40.9 ± 1.0	143.3±1.2	10.4 ± 1.1	1.2 ± 0.3	5.0 ± 3.3	3.5 ± 0.6	121 ± 6
CD200-10-0/6	28.8 ± 2.1	1.9 ± 0.1	9565.4	44,518.8 ± 5535.0	15,735.0 ± 1087.1	5359.6 ± 2479.4	3.5	1027.5 ± 298.6	341.2 ± 131.4	230 ± 30	19.2 ± 4.2	190 ± 48	1490 ± 20
CD200-360-0/6	27.3 ± 1.8	2.0 ± 0.1	11,292.0	54,222.0 ± 9737.7	18,429.3 ± 602.5	4226.9 ± 2928.9	189.0 ± 263.3	2356.9 ± 439.9	63.9 ± 19.1	260 ± 65	16.0 ± 4.1	60 ± 31	2180 ± 160
CD220-185-3	25.6 ± 0.5	2.2 ± 0.0	12,970.2	53,535.0± 1943.2	19,555.3 ± 671.9	2141.8 ± 492.8	3.1	1985.0 ± 99.0	60.8 ± 6.0	180 ± 62	8.3 ± 2.3	51 ± 8	1890 ± 360
CD240-10-0/6	27.3 ± 1.9	1.8 ± 0.1	10,753.2 ± 1330.7	101,258.3 ± 50,630.1	15,962.0 ± 435.4	3158.0 ± 1476.1	473.3 ± 618.1	2301.6 ± 530.4	112.9 ± 84.6	360 ± 81	8.1 ± 1.9	100 ± 80	1870 ± 240
CD240-360-0	22.5	2.5	-	110,882.0	20,862.4	4656.2	-	2172 .0	50.5	140	1.6	32	1470

3.6. PAH

The PAHs content in the biochar is dependent on the process conditions, mainly maximum temperature reached in the process, feedstock and mass transport limitations due to potential enhancement of heterogeneous secondary reactions. For example, as reported in [73], the emission of PAHs (detected in the vapor phase) for pine wood chips starts when the temperatures inside the solid bed range between 300–350 °C, being at those temperatures 2- and 3-ring aromatic compounds the main species. This is in good agreement with the results shown in Figure 7, where it is already observable that in the temperature range from 350–400 °C the highest amount of PAHs is present in the PW biochar, being phenanthrene the most significant species, as shown in Figure 7 (bottom left and right). However, as the temperature increases, the presence of PAHs decreases significantly. At those temperatures almost no more volatiles, which can further react within the solid matrix, are being produced and the temperatures are also high enough for a good part of the PAHs still present in the solid matrix to be removed. Inert gas flow rate may have also a significant impact on the formation of PAHs, since higher flow rates lead to lower volatiles concentration and retention time in the gas phase. Hence, the potential intraparticle heterogeneous secondary reactions may be reduced, main mechanism for PAHs formation at conversion temperatures lower than 500 °C [40,64,73]. This is further confirmed by results recently shown by Buss et al. [74].

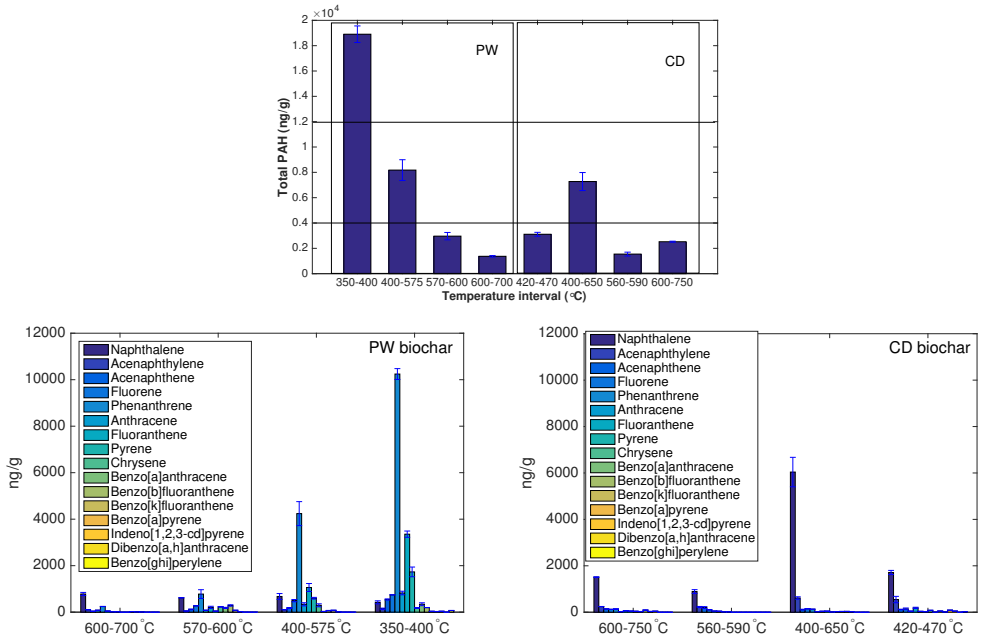

Figure 7. Top: Total content in PAHs (16 EPA PAHs) for PW and CD biochars. Horizontal lines correspond to the limits of PAHs content for basic (12 mg/kg) and premium (4 mg/kg) class biochars (EBC). **Bottom**: Content of PAHs species for PW and CD biochars.

For CD, however, the trend is not the same, since the highest contents in PAHs are shifted to higher temperatures, suggesting that the pathways behind their formation are different from the ones of PW biochar. This is further supported by their composition. In Figure 7, bottom left and right, it is shown that PAHs present in CD biochar are mainly naphthalene and acenaphthylene, while for PW biochars phenanthrene and fluoranthene are the main species at low temperatures. At high temperatures, naphthalene is the main species.

It must be taken also into account that the ash content in the CD biochar is very high, with values around 40% in mass, dry basis. Since the PAHs are produced in the organic phase, to compare the total PAHs in the same basis for CD and PW biochars (% mass, dry ash free basis), the PAHs content in the

case of CD should be multiplied by an approximate factor of 1.7. This leads to higher PAHs content, as function of the organic fraction, in CD than PW, except PW biochars produced at around 400 °C.

Regarding the application of biochar to soil, while in almost all cases a basic grade biochar is obtained, it can be concluded that for a high quality biochar temperatures close to 600 °C must be reached.

According to Schimmelpfennig and Glaser [21], hydrochars have very low total PAH content and low naphthalene/phenanthrene ratios, similar to PW biochars produced at low temperatures. Therefore, PAHs content in hydrochars should not be a major issue with respect to their application and they have not been measured in this study.

3.7. Wettability

In Figure 8, the water absorption behavior of several biochars is shown. On the top, those for PW biochars and, on the bottom, the behavior for CD biochars. CD biochars show increasing capacity in water absorption with higher conversion severity, probably due to an increase in porosity and reduction in surface functional groups. PW biochars present two completely different behaviors. While chars produced at the highest severity (600 °C, 40 NL min^{-1}) show similar patterns to those from CD biochars (although with slightly lower capacity to absorb water), those produced at lower temperatures do not show almost capacity to absorb water, reaching an asymptotic behavior after the first seconds.

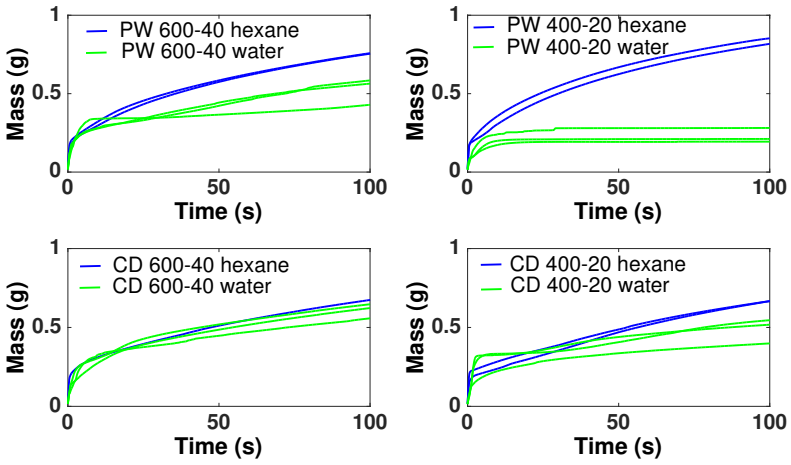

Figure 8. Water and hexane absorption curves of PW600-40, PW400-20, CD600-40, CD400-20.

When water is substituted by hexane, CD biochars still show similar absorption capacity in comparison to water, however the capacity of absorbing hexane by pine wood biochars is much higher than the one for water. If both absorption curves are compared, the contact angle can be determined, as explained in [50]. The contact angles obtained are shown in the Supplementary Material (Table S2). PW biochars present contact angles close to 90°, except PW600-40, while CD biochars present slightly lower contact angles. Although the theoretical definition of hydrophobicity is contact angle >90°, the fact that the values reported here are so close to 90° is an indication of high potential hydrophobicity [50]. From these results it can be concluded that biochars present mostly hydrophobic behavior, although this could be reduced with higher inert flow gas rates during the pyrolysis process, suggesting that a potential source of hydrophobicity is the condensation of volatiles on the char surface. It has been also shown in literature [50] that after one year in soil, biochars loose part of their hydrophobicity.

4. Conclusions

The influence of process conditions and feedsctock on several biochars and hydrochars properties has been studied in a comprehensive way and analyzed from mechanistic perspectives. This work

aims at contributing to biochar engineering, i.e., the capacity of designing and producing biochars able to perform a specific function for given soil, crop and climate requirements and constraints. Based on the current results, the following conclusions can be derived:

- Regarding primary characterization, biochars O/C molar ratio is linearly correlated to volatiles content, independently of the pyrolysis conditions and feedstock. However, H/C molar ratios of CD biochars are generally lower than those of PW biochars, which may be attributed to the higher inorganic matter content of CD, leading to different pyrolysis reaction pathways and enhancing aromatization. PW hydrochars H/C molar ratio and CD hydrochars O/C molar ratio are also outliers with respect to the linear behavior. This shows that elemental and proximate analysis are not enough to determine the chemical properties of biochars [19], due to the influence of feedstock properties on reaction pathways.
- The pH depends on both conversion process parameters and feedstock, having in general higher pH biochars and hydrochars produced from CD, with much higher inorganic content, including carbonates. In both PW and CD biochars pH correlates strongly with H/C molar ratio. PW biochars and PW hydrochars present also correlation with the O/C ratio. Only CD hydrochars show good correlation (r = 0.88) with the ash content. This shows that the H/C molar ratio may be a better indicator of surface chemistry than O/C ratios or volatiles content, which is also supported by measurements of the total acidic functional groups.
- The porous structure varies greatly among biochars. PW biochars produced at 600 °C present mainly microporosity with N_2-SSAs around 400 $m^2\ g^{-1}$. In CD biochars this microporosity is lower (<100 $m^2\ g^{-1}$). The significantly lower microporosity for all CD biochars is attributed to the high inorganic content, which could potentially block the micropores and enhance mesoporosity. PW and CD biochars produced at 400 °C present also micropores (as shown by CO_2 adsorption), but much less developed than at higher temperatures, i.e., microporosity must be still developed through volatiles release, to open the pores, and further solid aromatization. Furthermore, a higher N_2 sweeping flow during pyrolysis enhances microporosity (more than double for CD biochars at 600 °C). This indicates that micropores blocking is related to volatiles, which may further react to form secondary char or condense in the pores to a greater extent for lower flow rates, when the concentration and retention time of volatiles is higher. Hydrochars, on the contrary, present mainly mesoporosity, independently of the raw material and the process severity, having higher pore volume but generally lower SSA than biochars. Washing of hydrochars further increases the SSA and pore volume due to removal of condensed species.
- Regarding nutrients, NO_3^- and NH_4^+ availability is negligible after pyrolysis, irrespective of feedstock nitrogen content. The absolute availability of PO_4^{3-} is reduced compared to the feedstock. For PW biochars the relative availability increases with the pyrolysis conversion. Higher inert gas flow rate leads also to higher PO_4^{3-} availability. For hydrochars, HTC can potentially lead to an increase in availability of NO_3^-, NH_4^+, PO_4^{3-}, and K^+; however, these species are primarily solved in the process water. One exception is PO_4^{3-} which appears to form precipitates at higher concentration, i.e., for feedstocks with high direct nutrient potential. Similar to pyrolysis, there is the tendency that the availability of the investigated species is decreased at higher HTC temperatures.
- Biochars have a higher stability to oxidation than hydrochars. Besides the influence of process conditions, PW biochars show higher thermal stability than CD biochars. The same holds true for hydrochars. This may be related to the catalytic effect of AAEM during oxidation reactions.
- PAHs are already produced in biochars at temperatures as low as 340 °C. The maximum quantity is detected for temperatures around 400 °C, exceeding in the case of PW the maximum level for certification. At higher temperatures the PAHs content is reduced again due to vaporization of these species from the solid matrix, achieving a premium quality for temperatures above 550 °C. The composition of these species is highly dependent on the feedstock: naphthalene is the main

species in CD biochars, while phenanthrene and fluoranthene are the main species in PW biochars at low temperatures.

- Both PW and CD biochars present mostly a hydrophobic behavior, although it can be reduced with higher conversion temperatures and higher inert gas flow rates during pyrolysis, which reduces the extent of secondary reactions and recondesation of volatiles.

Based on the previous conclusions, the following general recommendations for biochar and hydrochar production can be derived. Pyrolysis temperatures above 550 °C guarantee low H/C and O/C ratios, PAHs content below the limit according to quality criteria (EBC), independently of the initial feedstock, higher SSAs and lower hydrophobicity. N_2 flow during pyrolysis can also contribute to further microporosity development and hydrophobicity reduction. High inorganic content in the feedstock potentially reduces SSA and hydrophobicity, but increases mesoporosity and pH. With respect to hydrochars, the EBC requirement regarding elemental composition can only be fulfilled for high temperature and residence times PW hydrochars. Hydrochars have a lower SSA than biochars, but a higher mesoporosity, total pore volume and nutrient availability. Washing of hydrochars after production further increases their surface area and pore volume. The results from this work can be applied to "engineer" appropriate biochars with respect to soil demands and certification requirements, as well as to improve biochar certification, and they are summarized in Figure 9.

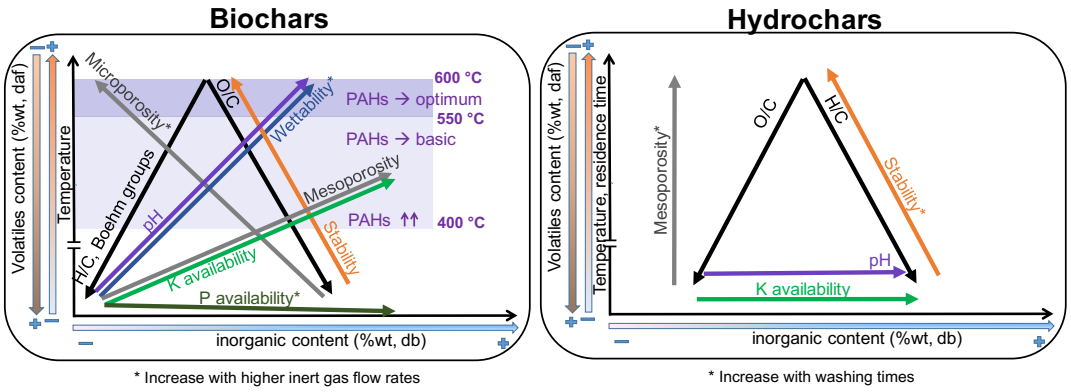

Figure 9. Conclusions. The direction of the arrows indicates increasing values for all properties.

Supplementary Materials: The following are available online at www.mdpi.com/1996-1073/11/3/496/s1.

Acknowledgments: The authors thank Susanne Hoffmann, Hernán Almuina Villar, Alba Domínguez Yebra, Alberto García Rueda and Christina Eichenauer (Technische Universität Berlin) for their support with the analytic characterization of biochars and hydrochars. The authors also thank the Leibniz Institute for Agricultural Engineering and Bioeconomy (Potsdam, Germany) for preparation of hydrochar samples. The authors acknowledge support by the German Research Foundation and the Open Access Publication Funds of Technische Universität Berlin.

Author Contributions: Alba Dieguez-Alonso, Axel Funke and Andrés Anca-Couce conceived and designed the experiments; Alba Dieguez-Alonso and Axel Funke performed the pyrolysis and hydrothermal carbonization experiments respectively; Alba Dieguez-Alonso, Axel Funke, Alessandro Girolamo Rombolà, Gerardo Ojeda and Jörg Bachmann analyzed the different biochar and hydrochar properties, with the further support from those mentioned in the acknowledgements; Alba Dieguez-Alonso, Andrés Anca-Couce, Axel Funke, Alessandro Girolamo Rombolà, Gerardo Ojeda and Jörg Bachmann and Frank Behrendt analyzed the data. Alba Dieguez-Alonso wrote the paper with important contributions from Andrés Anca-Couce and Axel Funke; the rest of the co-authors reviewed the manuscript and contributed to it when necessary according to their data analysis and interpretation. Frank Behrendt supervised the work.

Conflicts of Interest: The authors declare no conflict of interest.

Abbreviations

The following abbreviations are used in this manuscript:

CD	Corn digestate
PW	Pine wood
HTC	Hydrothermal carbonization
PSD	Pore size distribution
PAH	Polycyclic aromatic hydrocarbon
USEPA	United States Environmental Protection Agency

References

1. European Biochar Certificate (EBC). *European Biochar Certificate—Guidelines for Sustainable Production of Biochar*; Version 6.2E; European Biochar Foundation (EBC): Arbaz, Switzerland, 2012. Available online: http://www.europeanbiochar.org/en/download (accessed on 4 February 2016).
2. Standardized Product Definition and Product Testing Guidelines for Biochar That Is Used in Soil. International Biochar Intiative. Version 2.1. 2015. Available online: http://www.biochar-international.org/characterizationstandard (accessed on 19 October 2016).
3. Abiven, S.; Schmidt, M.; Lehmann, J. Biochar by design. *Nat. Geosci.* **2014**, *7*, 326–327.
4. Lee, M.E.; Park, J.H.; Chung, J.W. Adsorption of Pb(II) and Cu(II) by Ginkgo-Leaf-Derived Biochar Produced under Various Carbonization Temperatures and Times. *Int. J. Environ. Res. Public Health* **2017**, *14*, 1528.
5. Frišták, V.; Pipíška, M.; Soja, G. Pyrolysis treatment of sewage sludge: A promising way to produce phosphorus fertilizer. *J. Clean. Prod.* **2018**, *172*, 1772–1778.
6. Frišták, V.; Pipíška, M.; Lesný, J.; Soja, G.; Friesl-Hanl, W.; Packová, A. Utilization of biochar sorbents for Cd^{2+}, Zn^{2+}, and Cu^{2+} ions separation from aqueous solutions: Comparative study. *Environ. Monit. Assess.* **2014**, *187*, 4093, doi:10.1007/s10661-014-4093-y.
7. Inyang, M.I.; Gao, B.; Yao, Y.; Xue, Y.; Zimmerman, A.; Mosa, A.; Pullammanappallil, P.; Ok, Y.S.; Cao, X. A review of biochar as a low-cost adsorbent for aqueous heavy metal removal. *Crit. Rev. Environ. Sci. Technol.* **2016**, *46*, 406–433.
8. Mohan, D.; Sarswat, A.; Ok, Y.S.; Charles, U.P., Jr. Organic and inorganic contaminants removal from water with biochar, a renewable, low cost and sustainable adsorbent—A critical review. *Bioresour. Technol.* **2014**, *160*, 191–202.
9. Sohi, S.P.; Krull, E.; Lopez-Capel, E.; Bol, R. Chapter 2—A Review of Biochar and Its Use and Function in Soil. In *Advances in Agronomy*; Sparks, D.L., Ed.; Academic Press: Cambridge, MA, USA, 2010; Volume 105, pp. 47–82.
10. Chan, K.Y.; Xu, Z. Nutrient Properties and Their Enhancement. In *Biochar for Environmental Management. Science and Technology*; Earthscan: Abingdon, UK, 2009; Chapter 5, pp. 67–84, ISBN 978-1-84407-658-1.
11. Thies, J.E.; Rillig, M.C. Characteristics of Biochar: Biological Properties. In *Biochar for Environmental Management. Science and Technolgy*; Earthscan: Abingdon, UK, 2009; Chapter 6, pp. 85–105.
12. Anca-Couce, A.; Dieguez-Alonso, A.; Zobel, N.; Berger, A.; Kienzl, N.; Behrendt, F. Influence of Heterogeneous Secondary Reactions during Slow Pyrolysis on Char Oxidation Reactivity of Woody Biomass. *Energy Fuels* **2017**, *31*, 2335–2344.
13. Yuan, J.H.; Xu, R.K.; Zhang, H. The forms of alkalis in the biochar produced from crop residues at different temperatures. *Bioresour. Technol.* **2011**, *102*, 3488–3497.
14. Angst, T.E.; Sohi, S.P. Establishing release dynamics for plant nutrients from biochar. *GCB Bioenergy* **2013**, *5*, 221–226.
15. Zambon, I.; Colosimo, F.; Monarca, D.; Cecchini, M.; Gallucci, F.; Proto, R.A.; Lord, R.; Colantoni, A. An Innovative Agro-Forestry Supply Chain for Residual Biomass: Physicochemical Characterisation of Biochar from Olive and Hazelnut Pellets. *Energies* **2016**, *9*, 526.
16. Uchimiya, M.; Hiradate, S.; Antal, M.J. Dissolved Phosphorus Speciation of Flash Carbonization, Slow Pyrolysis, and Fast Pyrolysis Biochars. *ACS Sustain. Chem. Eng.* **2015**, *3*, 1642–1649.
17. Hossain, M.K.; Strezov, V.; Chan, K.Y.; Ziolkowski, A.; Nelson, P.F. Influence of pyrolysis temperature on production and nutrient properties of wastewater sludge biochar. *J. Environ. Manag.* **2011**, *92*, 223–228.

18. Mukherjee, A.; Zimmerman, A.; Harris, W. Surface chemistry variations among a series of laboratory-produced biochars. *Geoderma* **2011**, *163*, 247–255.
19. Budai, A.; Wang, L.; Gronli, M.; Strand, L.T.; Antal, M.J.; Abiven, S.; Dieguez-Alonso, A.; Anca-Couce, A.; Rasse, D.P. Surface Properties and Chemical Composition of Corncob and Miscanthus Biochars: Effects of Production Temperature and Method. *J. Agric. Food Chem.* **2014**, *62*, 3791–3799.
20. Lawrinenko, M.; Laird, D.A. Anion exchange capacity of biochar. *Green Chem.* **2015**, *17*, 4628–4636.
21. Schimmelpfennig, S.; Glaser, B. One step forward toward characterization: Some important material properties to distinguish biochars. *J. Environ. Qual.* **2011**, *42*, 1001–1013.
22. Zhao, S.X.; Ta, N.; Wang, X.D. Effect of Temperature on the Structural and Physicochemical Properties of Biochar with Apple Tree Branches as Feedstock Material. *Energies* **2017**, *10*, 1293.
23. Carrier, M.; Hardie, A.G.; Uras, A.; Görgens, J.; Knoetze, J.H. Production of char from vacuum pyrolysis of South-African sugar cane bagasse and its characterization as activated carbon and biochar. *J. Anal. Appl. Pyrolysis* **2012**, *96*, 24–32.
24. Gaskin, J.W.; Steiner, C.; Harris, K.; Das, K.C.; Bibens, B. Effect of low-temperature pyrolysis conditions on biochar for agricultural use. *Trans. ASABE* **2008**, *51*, 2061–2069.
25. Keiluweit, M.; Nico, P.S.; Johnson, M.G.; Kleber, M. Dynamic Molecular Structure of Plant Biomass-Derived Black Carbon (Biochar). *Environ. Sci. Technol.* **2010**, *44*, 1247–1253.
26. Cetin, E.; Moghtaderi, B.; Gupta, R.; Wall, T. Influence of pyrolysis conditions on the structure and gasification reactivity of biomass chars. *Fuel* **2004**, *83*, 2139–2150.
27. Downie, A.; Crosky, A.; Munroe, P. Physical Properties of Biochar. In *Biochar for Environmental Management. Science and Technology*; Earthscan: Abingdon, UK, 2009; Chapter 2, pp. 13–32, ISBN 978-1-84407-658-1.
28. Liu, Z.; Zhang, F.S.; Wu, J. Characterization and application of chars produced from pinewood pyrolysis and hydrothermal treatment. *Fuel* **2010**, *89*, 510–514.
29. Hagemann, N.; Joseph, S.; Schmidt, H.P.; Kammann, C.I.; Harter, J.; Borch, T.; Young, R.B.; Varga, K.; Taherymoosavi, S.; Elliott, K.W.; et al. Organic coating on biochar explains its nutrient retention and stimulation of soil fertility. *Nat. Commun.* **2017**, *8*, 1089, doi:10.1038/s41467-017-01123-0.
30. Van Zwieten, L.; Kimber, S.; Morris, S.; Chan, K.Y.; Downie, A.; Rust, J.; Joseph, S.; Cowie, A. Effects of biochar from slow pyrolysis of papermill waste on agronomic performance and soil fertility. *Plant Soil* **2010**, *327*, 235–246.
31. McCormack, S.A.; Ostle, N.; Bardgett, R.D.; Hopkins, D.W.; Vanbergen, A.J. Biochar in bioenergy cropping systems: Impacts on soil faunal communities and linked ecosystem processes. *GCB Bioenergy* **2013**, *5*, 81–95.
32. Antal, M.J.; Grønli, M. The Art, Science, and Technology of Charcoal Production. *Ind. Eng. Chem. Res.* **2003**, *42*, 1619–1640.
33. Brassard, P.; Godbout, S.; Raghavan, V.; Palacios, H.J.; Grenier, M.; Zegan, D. The Production of Engineered Biochars in a Vertical Auger Pyrolysis Reactor for Carbon Sequestration. *Energies* **2017**, *10*, 288.
34. Titirici, M.M.; White, R.J.; Falco, C.; Sevilla, M. Black perspectives for a green future: Hydrothermal carbons for environment protection and energy storage. *Energy Environ. Sci.* **2012**, *5*, 6796–6822.
35. Huff, M.D.; Kumar, S.; Lee, J.W. Comparative analysis of pinewood, peanut shell, and bamboo biomass derived biochars produced via hydrothermal conversion and pyrolysis. *J. Environ. Manag.* **2014**, *146*, 303–308.
36. Cao, X.; Ro, K.S.; Chappell, M.; Li, Y.; Mao, J. Chemical Structures of Swine-Manure Chars Produced under Different Carbonization Conditions Investigated by Advanced Solid-State 13C Nuclear Magnetic Resonance (NMR) Spectroscopy. *Energy Fuels* **2011**, *25*, 388–397.
37. Wiedner, K.; Naisse, C.; Rumpel, C.; Pozzi, A.; Wieczorek, P.; Glaser, B. Chemical modification of biomass residues during hydrothermal carbonization—What makes the difference, temperature or feedstock? *Org. Geochem.* **2013**, *54*, 91–100.
38. Busch, D.; Stark, A.; Kammann, C.I.; Glaser, B. Genotoxic and phytotoxic risk assessment of fresh and treated hydrochar from hydrothermal carbonization compared to biochar from pyrolysis. *Ecotoxicol. Environ. Saf.* **2013**, *97*, 59–66.
39. Busch, D.; Glaser, B. Stability of co-composted hydrochar and biochar under field conditions in a temperate soil. *Soil Use Manag.* **2015**, *31*, 251–258.
40. Dieguez-Alonso, A.; Anca-Couce, A.; Zobel, N. On-line tar characterization from pyrolysis of wood particles in a technical-scale fixed-bed reactor by applying Laser-Induced Fluorescence (LIF). *J. Anal. Appl. Pyrolysis* **2013**, *102*, 33–46.

41. Naumann, C.; Bassler, R.; Seibold, R.; Barth, C. *Methodenbuch. Band III, Die Chemische Untersuchung von Futtermitteln*; VDLUFA-Verlag: Darmstadt, Germany, 1997.
42. Boehm, H.P.; Diehl, E.; Heck, W.; Sappok, R. Surface Oxides of Carbon. *Angew. Chem. Int. Ed.* **1964**, *3*, 669–677.
43. Goertzen, S.L.; Theriault, K.D.; Oickle, A.M.; Tarasuk, A.C.; Andreas, H.A. Standardization of the Boehm titration. Part I. CO_2 expulsion and endpoint determination. *Carbon* **2010**, *48*, 1252–1261.
44. Tsechansky, L.; Graber, E.R. Methodological limitations to determining acidic groups at biochar surfaces via the Boehm titration. *Carbon* **2014**, *66*, 730–733.
45. Brunauer, S.; Emmett, P.H.; Teller, E. Adsorption of Gases in Multimolecular Layers. *J. Am. Chem. Soc.* **1938**, *60*, 309–319.
46. Barrett, E.P.; Joyner, L.G.; Halenda, P.P. The Determination of Pore Volume and Area Distributions in Porous Substances. I. Computations from Nitrogen Isotherms. *J. Am. Chem. Soc.* **1951**, *73*, 373–380.
47. Seaton, N.; Walton, J.; Quirke, N. A new analysis method for the determination of the pore-size distribution of porous carbons from nitrogen adsorption measurements. *Carbon* **1989**, *27*, 853–861.
48. Hoffmann, G. *Methodenbuch. Band I, Die Untersuchung von Böden*; VDLUFA-Verlag: Darmstadt, Germany, 1991.
49. Fabbri, D.; Rombola, A.G.; Torri, C.; Spokas, K.A. Determination of polycyclic aromatic hydrocarbons in biochar and biochar amended soil. *J. Anal. Appl. Pyrolysis* **2013**, *103*, 60–67.
50. Ojeda, G.; Mattana, S.; Avila, A.; Alcaniz, J.M.; Volkmann, M.; Bachmann, J. Are soil-water functions affected by biochar application? *Geoderma* **2015**, *249–250*, 1–11.
51. Krull, E.S.; Baldock, J.A.; Skjemstad, J.O.; Smernik, R.J. Characteristics of Biochar: Organo-Chemical Properties. In *Biochar for Environmental Management. Science and Technology*; Earthscan: Abingdon, UK, 2009; Chapter 4, pp. 53–65, ISBN 978-1-84407-658-1.
52. Rombolà, A.G.; Fabbri, D.; Meredith, W.; Snape, C.E.; Dieguez-Alonso, A. Molecular characterization of the thermally labile fraction of biochar by hydropyrolysis and pyrolysis-GC/MS. *J. Anal. Appl. Pyrolysis* **2016**, *121*, 230–239.
53. Mumme, J.; Eckervogt, L.; Pielert, J.; Diakité, M.; Rupp, F.; Kern, J. Hydrothermal carbonization of anaerobically digested maize silage. *Bioresour. Technol.* **2011**, *102*, 9255–9260.
54. Li, F.; Cao, X.; Zhao, L.; Wang, J.; Ding, Z. Effects of Mineral Additives on Biochar Formation: Carbon Retention, Stability, and Properties. *Environ. Sci. Technol.* **2014**, *48*, 11211–11217.
55. Liu, W.J.; Jiang, H.; Yu, H.Q. Development of Biochar-Based Functional Materials: Toward a Sustainable Platform Carbon Material. *Chem. Rev.* **2015**, *115*, 12251–12285.
56. Yin, S.; Mehrotra, A.K.; Tan, Z. Alkaline hydrothermal conversion of cellulose to bio-oil: Influence of alkalinity on reaction pathway change. *Bioresour. Technol.* **2011**, *102*, 6605–6610.
57. Pulido-Novicio, L.; Hata, T.; Kurimoto, Y.; Doi, S.; Ishihara, S.; Imamura, Y. Adsorption capacities and related characteristics of wood charcoals carbonized using a one-step or two-step process. *J. Wood Sci.* **2001**, *47*, 48–57.
58. Nguyen, B.T.; Lehmann, J. Black carbon decomposition under varying water regimes. *Org. Geochem.* **2009**, *40*, 846–853.
59. Baldock, J.A.; Smernik, R.J. Chemical composition and bioavailability of thermally altered *Pinus resinosa* (Red pine) wood. *Org. Geochem.* **2002**, *33*, 1093–1109.
60. Lee, J.W.; Kidder, M.; Evans, B.R.; Paik, S.; Buchanan, A.C., III; Garten, C.T.; Brown, R.C. Characterization of Biochars Produced from Cornstovers for Soil Amendment. *Environ. Sci. Technol.* **2010**, *44*, 7970–7974.
61. Ronsse, F.; van Hecke, S.; Dickinson, D.; Prins, W. Production and characterization of slow pyrolysis biochar: Influence of feedstock type and pyrolysis conditions. *GCB Bioenergy* **2013**, *5*, 104–115.
62. Yang, F.; Zhao, L.; Gao, B.; Xu, X.; Cao, X. The Interfacial Behavior between Biochar and Soil Minerals and Its Effect on Biochar Stability. *Entviron. Sci. Technol.* **2016**, *50*, 2264–2271.
63. Guizani, C.; Jeguirim, M.; Valin, S.; Limousy, L.; Salvador, S. Biomass Chars: The Effects of Pyrolysis Conditions on Their Morphology, Structure, Chemical Properties and Reactivity. *Energies* **2017**, *10*, 796.
64. Anca-Couce, A. Reaction mechanisms and multi-scale modelling of lignocellulosic biomass pyrolysis. *Prog. Energy Combust. Sci.* **2016**, *53*, 41–79.
65. Harvey, O.R.; Kuo, L.J.; Zimmerman, A.R.; Louchouarn, P.; Amonette, J.E.; Herbert, B.E. An Index-Based Approach to Assessing Recalcitrance and Soil Carbon Sequestration Potential of Engineered Black Carbons (Biochars). *Environ. Sci. Technol.* **2012**, *46*, 1415–1421.

66. Kuo, L.J.; Herbert, B.E.; Louchouarn, P. Can levoglucosan be used to characterize and quantify char/charcoal black carbon in environmental media? *Org. Geochem.* **2008**, *39*, 1466–1478.
67. Plante, A.F.; Fernández, J.M.; Haddix, M.L.; Steinweg, J.M.; Conant, R.T. Biological, chemical and thermal indices of soil organic matter stability in four grassland soils. *Soil Biol. Biochem.* **2011**, *43*, 1051–1058.
68. Zimmerman, A.R. Abiotic and Microbial Oxidation of Laboratory-Produced Black Carbon (Biochar). *Environ. Sci. Technol.* **2010**, *44*, 1295–1301.
69. Funke, A. Fate of Plant Available Nutrients during Hydrothermal Carbonization of Digestate. *Chem. Ing. Tech.* **2015**, *87*, 1713–1719.
70. Singh, B.; Singh, B.P.; Cowie, A.L. Characterisation and evaluation of biochars for their application as a soil amendment. *Aust. J. Soil Res.* **2010**, *48*, 516–525.
71. Funke, A.; Mumme, J.; Koon, M.; Diakité, M. Cascaded production of biogas and hydrochar from wheat straw: Energetic potential and recovery of carbon and plant nutrients. *Biomass Bioenergy* **2013**, *58*, 229–237.
72. Kruse, A.; Koch, F.; Stelzl, K.; Wüst, D.; Zeller, M. Fate of Nitrogen during Hydrothermal Carbonization. *Energy Fuels* **2016**, *30*, 8037–8042.
73. Dieguez-Alonso, A.; Anca-Couce, A.; Zobel, N.; Behrendt, F. Understanding the primary and secondary slow pyrolysis mechanisms of holocellulose, lignin and wood with laser-induced fluorescence. *Fuel* **2015**, *153*, 102–109.
74. Buss, W.; Graham, M.C.; MacKinnon, G.; Masek, O. Strategies for producing biochars with minimum {PAH} contamination. *J. Anal. Appl. Pyrolysis* **2016**, *119*, 24–30.